

# A Rationale for the Linear Correlation of Aryl Substituent Effects in Iron(0) Tricarbonyl Complexes Containing $\alpha,\beta$ -Unsaturated Enone (Chalcone) Ligands

Benjamin E. Moulton, Anne K. Duhme-Klair, Ian J. S. Fairlamb,\* Jason M. Lynam,\* and Adrian C. Whitwood

Department of Chemistry, University of York, Heslington, York, YO10 5DD, U.K.

Received June 26, 2007

A library of iron(0) tricarbonyl complexes containing  $\eta^4$ -bound  $\alpha,\beta$ -unsaturated enone ligands [ $\text{Fe}(\text{CO})_3(\eta^4\text{-RCH}=\text{CH}-\text{C}\{\text{Ph}\}=\text{O})$ ] has been prepared to facilitate comprehensive correlation of the electronic withdrawing/donating properties of the substituent, R, with the strength of the metal–ligand interaction. The IR and NMR spectroscopic data proved invaluable in aiding a comprehensive correlation and global understanding of the aryl substituent effects. The frequency of the M–CO bands in the infrared spectra of these species exhibits a linear correlation with the Hammett parameters for the substituents. The coordination shifts in both the  $^1\text{H}$  and  $^{13}\text{C}$  NMR spectra for the ligands exhibit a similar linear relationship. The largest coordination shifts are observed when more electron-withdrawing groups are present, implying that the organic ligand is primarily acting as a  $\pi$ -acid. The structures of six complexes of this type have been determined by single-crystal X-ray diffraction.

## Introduction

The ability of the steric and electronic properties of ligands to modulate the reactivity of metal complexes is a well-documented phenomenon. A common example of how these effects may be quantified is the system developed by Tolman in which the steric and electronic properties of phosphorus(III) ligands could be quantified.<sup>1</sup> The steric bulk of these ligands may be evaluated by the cone angle parameter and the electronic properties by coordination of the ligand to a suitable metal carbonyl complex and observing the changes in the infrared spectra of the CO bands. Therefore, both the steric and electronic effects of phosphorus(III) ligands may be easily rationalized, and this approach has had a considerable impact in the utilization of these ligands in, for example, palladium-catalyzed cross-coupling reactions, as the electron density and topology of the metal complexes can be controlled.<sup>2</sup>

Although these relationships are now well-established for phosphorus(III)-containing ligands, there is less quantitative experimental information available on the effects of the systematic manipulation of the electronic and/or steric structure of organic frameworks on metal–ligand bonding. Furthermore, given that the majority of  $\pi$ -ligands bind to metals through a series of synergic donor/acceptor interactions, it is somewhat difficult to rationalize *a priori* which of these two effects will dominate the metal–ligand interactions. Our primary interest in this study is based on recent work on metal complexes of iron(0),<sup>3</sup> iron(II), and molybdenum(II)<sup>4</sup> containing  $\pi$ -acidic diene

ligands (e.g., 2-pyrones). In studies in parallel to this, one of us (I.J.S.F.) has tuned  $\pi$ -acidic dibenzylidene acetone (dba), enone-type ligands, and coordinated these to palladium(0).<sup>5</sup> Dramatic effects on catalytic activity are observed in various palladium(0)-catalyzed cross-coupling processes on making very subtle structural changes to the aryl groups of dba. Wishing to gain further understanding of the interaction of enone-type ligands with low-valent metal centers, we have correlated comprehensively the substituent effects of a series of iron(0) tricarbonyl complexes containing  $\eta^4$ -bound  $\alpha,\beta$ -unsaturated ketone ligands in order to gauge if the relative importance of the donor/acceptor interactions may be quantified. By varying the substituents on the aryl ring connected directly to the enone  $\pi$ -system of the chalcone, both the inductive and mesomeric effects of the substituents may be probed. As the complexes [ $\text{Fe}(\text{CO})_2\text{L}(\eta^4\text{-PhCH}=\text{CH}-\text{C}\{\text{Me}\}=\text{O})$ ] (L = phosphorus-containing ligand) have been used to explore the effect of the phosphorus ligands on metal–ligand binding<sup>6</sup> and redox chemistry,<sup>7</sup> we reasoned that these species would be a good framework to test our hypothesis. Species such as [ $\text{Fe}(\text{CO})_3(\eta^4\text{-PhCH}=\text{CH}-\text{C}\{\text{Me}\}=\text{O})$ ] have been used as transfer reagents for the  $\text{Fe}(\text{CO})_3$  group, and a precise understanding of metal–ligand bonding might enable the design of ligands that will act as better leaving groups.<sup>8</sup> Furthermore, these species have proven to be versatile reagents for the preparation of 1,4-diketones<sup>9</sup> and optically pure ketones,<sup>10</sup> as well as iron(0) vinyl ketene,<sup>11</sup> vinyl ketenimine,<sup>11b,12</sup> and triene complexes,<sup>11b</sup> which are also useful synthetic precursors.<sup>13</sup>

A range of diaryl-substituted  $\alpha,\beta$ -unsaturated ketones (referred herein by their historical name of *chalcones*) can be prepared by Claisen-Schmidt condensation of acetophenone with an

(1) Tolman, C. *Chem. Rev.* **1977**, *77*, 313.

(2) See for example: Andersen, N. G.; Keay, B. A. *Chem. Rev.* **2001**, *101*, 997.

(3) (a) Fairlamb, I. J. S.; Syv anne, S. M.; Whitwood, A. C. *Synlett* **2003**, 1673. (b) Fairlamb, I. J. S.; Motterlini, R.; Duhme-Klair, A.-K.; Lynam, J. M.; et al. *Bioorg. Med. Chem. Lett.* **2006**, *16*, 995. (c) Sawle, P.; Hammad, J.; Fairlamb, I. J. S.; Moulton, B. E.; O'Brien, C. T.; Lynam, J. M.; Duhme-Klair, A. K.; Foresti, R.; Motterlini, R. *J. Pharmacol. Exper. Ther.* **2006**, *318*, 403.

(4) Fairlamb, I. J. S.; Lynam, J. M.; Taylor, I. E.; Whitwood, A. C. *Organometallics* **2004**, *21*, 4964.

(5) (a) Fairlamb, I. J. S.; Kapdi, A. R.; Lee, A. F. *Org. Lett.* **2004**, *6*, 4435. Fairlamb, I. J. S.; Kapdi, A. R.; Lee, A. F.; McGlacken, G. P.; Weissburger, F.; de Vries, A. H. M.; Schmieder-van de Vondervoort, L. *Chem.–Eur. J.* **2006**, *12*, 8750. (b) Fairlamb, I. J. S.; Jutand, A.; Mac e, Y.; Kapdi, A. R. *Organometallics* **2006**, *25*, 1795.

(6) Vichi, E. J. S.; Fujiwara F. Y.; Stein, E. *Inorg. Chem.* **1985**, *24*, 286.

(7) Vichi, E. J. S.; Stein, E. *Inorg. Chem. Acta* **2002**, *334*, 313.

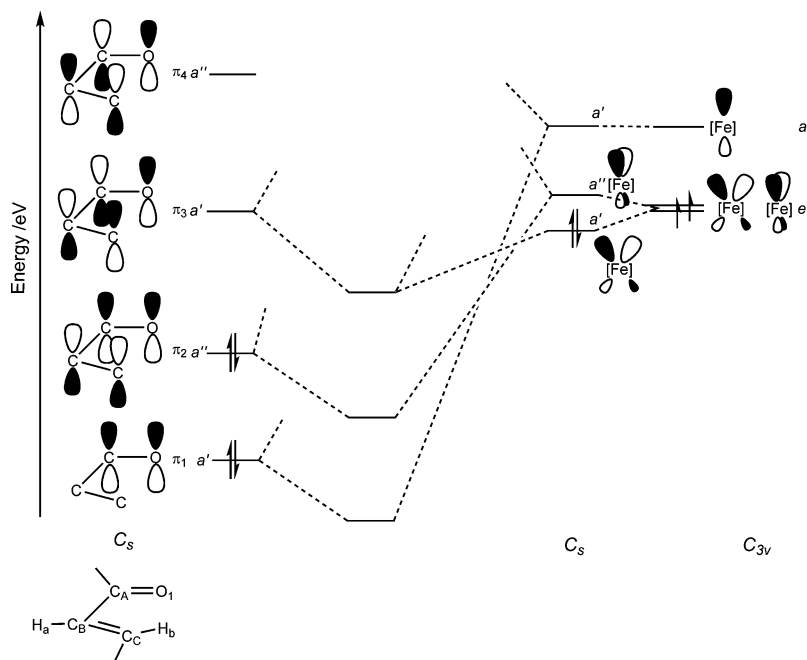


**Figure 1.** Partial qualitative MO diagram illustrating the major bonding interactions between an  $\alpha,\beta$ -unsaturated enone and an iron(0) tricarbonyl fragment. The  $C_s$  symmetry labels refer to the pseudomirror plane perpendicular to  $C_A-C_B$ . [Fe] =  $\text{Fe}(\text{CO})_3$ .

appropriately substituted benzaldehyde. Coordination to iron(0) can then be achieved by reaction with  $[\text{Fe}_2(\text{CO})_9]$  in ethereal solvents.<sup>14–16</sup> Given that the Hammett parameters for the substituents on the aryl ring connected to the  $\text{C}=\text{C}$  unit in the chalcone are readily available,<sup>17</sup> the changes in the IR and NMR spectra of these compounds could be correlated with these

electronic parameters. In turn, this has facilitated a quantitative assessment of the changes on the metal–ligand bonding interactions in terms of the net donor/acceptor character of the ligand.

The bonding between the  $\text{Fe}(\text{CO})_3$  fragment<sup>18</sup> and the  $\alpha,\beta$ -unsaturated ketone ligand<sup>19</sup> may be rationalized in terms of the molecular orbitals shown in Figure 1. The four frontier molecular orbitals (FMOs) of the chalcone exhibit significant deviancy when compared to their isoelectronic 1,3-butadiene analogues. It has been calculated that the asymmetry introduced into the bonding by the electronegative oxygen atom results in the HOMO–1 ( $\pi_1$ ) being dominated almost solely by the  $p_z$ -orbitals on  $\text{O}_1$  and  $\text{C}_A$ : the oxygen-based orbitals contribute to a lesser extent to the higher energy FMOs.<sup>19</sup> On coordination of the chalcone to the metal center, the degeneracy of the half-filled HOMO of  $\text{Fe}(\text{CO})_3$  having e-symmetry is broken with the orbital, which is dominated by a contribution from  $d_{xz}$ , lowered in energy. This is of the correct symmetry to donate electrons into the vacant  $\pi_3$ -orbital on the chalcone, with the ligand acting as a  $\pi$ -acceptor. The effect of this donation is a decrease in the  $\text{C}_B-\text{C}_C$  and  $\text{C}_A-\text{O}_1$  bond order but an increase in the  $\text{C}_A-\text{C}_B$  bond order. The second orbital, formerly of e-symmetry, is dominated by a contribution from  $d_{yz}$  and is raised in energy compared to the parent orbital. The ligand-based  $\pi_2$ -orbital acts as a  $\pi$ -donor into this orbital. The resulting depopulation of the  $\pi_2$ -orbital (which is bonding between  $\text{C}_B$  and  $\text{C}_C$  and between  $\text{C}_A$  and  $\text{O}_1$ , but antibonding between  $\text{C}_A$  and  $\text{C}_B$ ) will have the same precise effect on the trends of the bond orders (and therefore bond lengths) within the chalcone framework as the previous interaction when the ligand acts as a  $\pi$ -acceptor through  $\pi_3$ .

In essence, the interplay between these two interactions, which mutually reinforce one another, highlights the problems associ-

- (8) (a) Howell, J. A. S.; Johnson, B. F. G.; Josty, P. L.; Lewis, J. J. *Organomet. Chem.* **1972**, *39*, 329. (b) Johnson, B. F. G.; Lewis, J.; Stephenson G. R.; Vichi, E. J. S. *J. Chem. Soc., Dalton Trans.* **1978**, 369. (c) Graham, C. R.; Scholes, G.; Brookhart, M. *J. Am. Chem. Soc.* **1977**, *99*, 1180. (d) Howell, J. A. S.; Burkinshaw, P. M. *J. Organomet. Chem.* **1978**, *152*, C5. (e) Evans, G.; Johnson, B. F. G.; Lewis, J. J. *Organomet. Chem.* **1975**, *102*, 507. (f) D. H. R. Barton, D. H. R.: A. A. Gunatilaka, A. A.; Nakanishi, T.; Patin, H.; Widdowson, D. A.; Worth, B. R. *J. Chem. Soc., Perkin Trans. 1* **1976**, 821. (g) Paquette, L. A.; Photis J. M.; Ewing, G. D. *J. Am. Chem. Soc.* **1975**, *97*, 3538. (h) Brookhart, M.; Nelson, G. O.; Scholes, G.; Watson, R. A. *J. Chem. Soc., Chem. Commun.* **1976**, 195. (i) Santini, C. C.; Fischer, J.; Mathey F.; Mitschler, A. *Inorg. Chem.* **1981**, *20*, 2428. (j) Birch, A. J.; Raverty, W. D.; Stephenson, G. R. *Tetrahedron Lett.* **1980**, *21*, 197. (k) Birch, A. J.; Raverty W. D.; Stephenson, G. R. *Organometallics* **1984**, *3*, 1057. (l) Domingos, J. P.; Howell, J. A. S.; Johnson, B. F. G.; Lewis, J. *Inorg. Synth.* **1976**, *16*, 103. (m) Fleckner, H.; Grevels, F. W.; Hess, D. *J. Am. Chem. Soc.* **1984**, *106*, 2027.

- (9) (a) Thomas, S. E. *J. Chem. Soc., Chem. Commun.* **1987**, 226. (b) Kitahara, H.; Tozawa, Y.; Fujita, S.; Tajiri, A.; Monta N.; Asao, T. *Bull. Chem. Soc. Jpn.* **1988**, 3362.

- (10) Zhang, W. Y.; Jakiela, D. J.; Maul, A.; Knors, C.; Lauber, J. W.; Helquist P.; Enders, D. *J. Am. Chem. Soc.* **1988**, *110*, 4652.

- (11) (a) Alcock, N. W.; Danks T. N.; Richards C. J.; Thomas, S. E. *J. Chem. Soc., Chem. Commun.* **1989**, 21. (b) Alcock, N. W.; Richards C. J.; Thomas, S. E. *Organometallics* **1991**, *10*, 231. (c) Benyunes S. A.; Thomas, S. E. *J. Chem. Soc., Chem. Commun.* **1996**, 43. (d) Garcia-Mellado, R.; Gutierrez-Perez, C.; Alvarez-Toledano, R.; Toscano, A.; Cabrera, A. *Polyhedron* **1997**, *16*, 2979.

- (12) Richards C. J.; Thomas, S. E. *J. Chem. Soc., Chem. Commun.* **1990**, 307.

- (13) (a) Hill, L.; Richards, C. J.; Thomas, S. E. *J. Chem. Soc., Chem. Commun.* **1990**, 1085. (b) Hill, L.; Richards C. J.; Thomas, S. E. *Pure Appl. Chem.* **1990**, *62*, 2066. (c) Hill, L.; Saberi, S. P.; Slawin, A. M. Z.; Thomas, S. E.; Williams, D. E. *J. Chem. Soc., Chem. Commun.* **1991**, 1290. (d) Saberi S. P.; Thomas, S. E. *J. Chem. Soc., Perkin Trans. 1* **1992**, 259. (e) Morris, K. G.; Saberi, S. P.; Salwin, A. M. Z.; Thomas, S. E. *J. Chem. Soc., Chem. Commun.* **1992**, 1789. (f) Morris, K. G.; Saberi S. P.; Thomas, S. E. *J. Chem. Soc., Chem. Commun.* **1993**, 209.

- (14) Stark, K.; Lancaster, J. E.; Murdoch, H. D.; Weiss, E. Z. *Naturforsch.* **1964**, *19b*, 284.

- (15) Brodie, A. M.; Johnson, B. F. G.; Joshy, P. L.; Lewis, J. J. *Chem. Soc., Dalton Trans.* **1972**, 2031.

- (16) Gibson (née Thomas), S. E.; Tustin, G. J. *J. Chem. Soc., Perkin Trans. 1* **1995**, 2427.

- (17) Okamoto, Y.; Brown, H. C. *J. Org. Chem.* **1957**, *22*, 485–494.

- (18) (a) Elian, M.; Hoffmann, R. *Inorg. Chem.* **1975**, *14*, 1058. (b) Elian, M.; Chen, M. L. C.; Mingos, D. M. P.; Hoffmann, R. *Inorg. Chem.* **1976**, *15*, 1148. (c) Mingos, D. M. P. *J. Chem. Soc., Dalton Trans.* **1977**, 20.

- (19) Calhorda M. J.; Vichi, E. J. S. *Organometallics* **1990**, *9*, 1060.

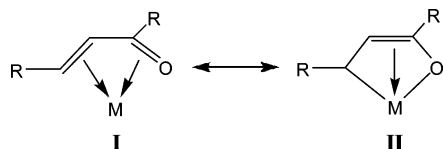


**Figure 2.** Resonance forms to describe the bonding in the  $\alpha,\beta$ -unsaturated ketone complexes.

ated with determining which dominates the bonding in enone based  $\pi$ -ligands. The remainder of the bonding between the metal and the ligand is constructed from a combination of the vacant orbital of a-type symmetry on the metal with  $\pi_1$ .

An alternative way to view the bonding between the metal and the chalcone ligand is through the two canonical forms **I** and **II** (Figure 2). In resonance form **I** the iron may be considered to be in the zero oxidation state; in resonance form **II** the metal has undergone a formal two-electron oxidation and the ligand may be considered to be bonding via an  $sp^3$ -bonded carbon with the central two carbon atoms of the ligand now bound to the metal as an alkene.

## Results and Discussion

**a. Synthesis of Ligands and Complexes.** In order to probe the effect of the electronic properties of the chalcone ligands on the resulting iron(0) complexes, a series of chalcones was prepared by Claisen-Schmidt condensation of appropriately substituted benzaldehyde and acetophenone in an ethanolic solution of NaOH (Scheme 1). The range of chalcones prepared, with the labeling scheme employed throughout this paper, is presented in Table 1. The ligands can be coordinated to iron(0) by heating at reflux with  $Fe_2(CO)_9$  in  $Et_2O$  solution for 16 h. The complexes were all obtained as orange-red air-stable solids in good to modest yields.

**b. Characterization.** Although complexes of the general type  $[Fe(CO)_3(\eta^4-RCH=CH-C\{R'\}=O)]$  have been known for some time and are well-characterized,<sup>14,15</sup> it is instructive to discuss the pertinent spectroscopic characteristics of these compounds so that the following systematic trends may be placed into context.

The infrared spectra of all of the complexes in  $CH_2Cl_2$  solution exhibit two strong bands and one weak band in the region typical of metal carbonyl stretches. This indicates that, in solution, the complex is approximating  $C_{3v}$ -symmetry due to rapid rotation around the  $Fe(CO)_3$  chalcone axis, an effect that is also observed in the  $^{13}C\{^1H\}$  NMR spectra (*q.v.*). No band in the region  $1600\text{--}1700\text{ cm}^{-1}$  was observed, indicating that the  $C=O$  unit of the chalcone ligand is coordinated to the metal.<sup>15</sup>

The  $^1H$  NMR spectra of the complexes exhibit significant changes when compared to the spectra of the free ligand. Principally, the resonances for the two protons of the vinyl group  $H_a$  and  $H_b$  both exhibit significant shifts to higher field when compared with the resonances of corresponding protons in the free ligand. For example, for the parent chalcone system  $PhCH=CH-C(Ph)=O$ , the resonance for  $H_b$  is observed at  $\delta$  7.82 in the free ligand (**1a**): in complex **2a** this resonance is observed at  $\delta$  3.45. A coordination shift is also observed for  $H_a$ , although

it is of a smaller magnitude ( $\delta_{free}$  7.54,  $\delta_{complex}$  6.73), and the coupling constant  $^3J_{HH}$  between the two hydrogen atoms decreases on complexation from 15.8 Hz to 9.1 Hz. The observed changes seen in the NMR spectra on coordination are as would be predicted on the basis of the model used to describe the interaction between the chalcone and the metal. If one considers the bonding within the complex to be a combination of resonance forms **I** and **II** (Figure 2), then it is clear that, in both forms,  $H_a$  is attached to an  $sp^2$ -carbon atom, hence the small change in chemical shift on coordination. In contrast,  $H_b$  is attached to an  $sp^3$ -hybridized carbon atom in resonance form **II**, thus explaining the larger shift on coordination.

The changes observed in the  $^{13}C\{^1H\}$  NMR spectrum of **2a** show identical patterns with a coordination shift of  $C_B$  of  $\Delta\delta$  48.0 and for  $C_C$  at  $\Delta\delta$  82.5. Consistent with the coordination of the carbonyl group to the metal, no resonances were observed in the spectrum between  $\delta$  190 and 160. Furthermore, at room temperature, no resonances that could be assigned to the metal carbonyls were observed, even after extended acquisition times coupled with long recycle delays. On lowering the temperature of the sample to 285 K, three resonances could be observed in the region typical of metal carbonyl groups (Figure 3).

This suggests that a fluxional process is occurring, consistent with a turnstile rotation around the  $Fe(CO)_3$  chalcone axis.<sup>20</sup> A similar effect has been reported in the  $^{13}C$  NMR spectra of the related compound  $[Fe(CO)_3(\eta^4-PhCH=CH-C\{Me\}=O)]$ .<sup>6</sup> Assuming that the coalescence temperature for this process is 300 K,<sup>21</sup> the activation barrier for **2a** is calculated to be 13.0 kcal  $mol^{-1}$ ,<sup>22</sup> similar to that reported for  $[Fe(CO)_3(\eta^4-PhCH=CH-C\{H\}=O)]$ .<sup>23</sup> Comprehensive studies by Knölker and co-workers<sup>24</sup> showed that such fluxionality was observed in the  $^{13}C$  NMR spectra of azabuta-1,3-diene complexes of  $Fe(CO)_3$ . Here it was demonstrated that the  $Fe(CO)_3$  group undergoes a temperature-dependent turnstile-type rotation with barriers of rotation between 13.5 and 14.7 kcal  $mol^{-1}$ .

The mass spectra of the complexes, recorded using the FAB technique in a matrix of 3-nitrobenzyl alcohol (3-NOBA), showed weak peaks for the expected pseudomolecular ion ( $MH^+$ ): further ion peaks were observed due to sequential loss of carbonyl ligands. In addition a peak was observed at  $m/z$  68 mass units higher than the expected molecular ion for all of the complexes, and it is suggested that this peak is due to decomposition of the complex in the matrix and formation of  $Fe(\eta^4-RCH=CH-C\{Ph\}=O)(\eta^6-3-NOBA)$ , **3**, Figure 4. The peak was not observed on changing the matrix to 2-nitrophenyl ether (2-NOPE), nor was the peak for the molecular ion. An accurate mass determination for this peak in complex **2c** was consistent with the formation of  $[Fe(\eta^4-4-MeO-C_6H_4CH=CH-C\{Ph\}=O)(\eta^6-3-NOBA)]^+$ . The independent preparation of these compounds has been attempted without success.

To assess the effects of the substituents in the chalcone ligand on the bonding between the metal and the complex, the data gathered *vide supra* has been analyzed comprehensively.

**c. Systematic Trends.** The IR spectra of all of the complexes were recorded in  $CH_2Cl_2$  solution. Table 1 shows the Hammett  $\sigma$ -values and the frequency of the bands due to the  $C-O$

**Scheme 1.** Synthesis of Chalcone Ligands and Iron(0) Tricarbonyl Complexes

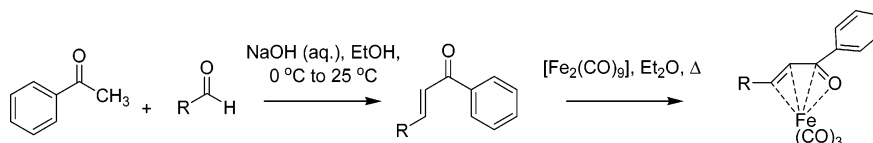
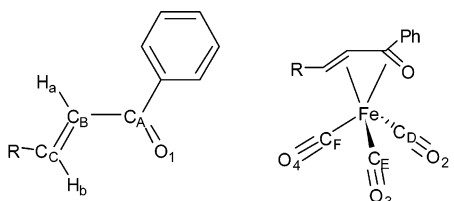
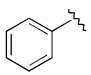
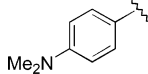
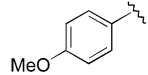
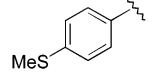
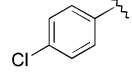
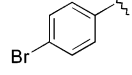
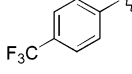
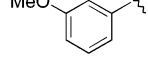
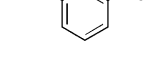
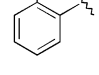
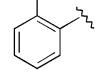
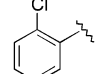
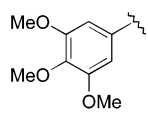
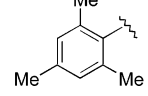
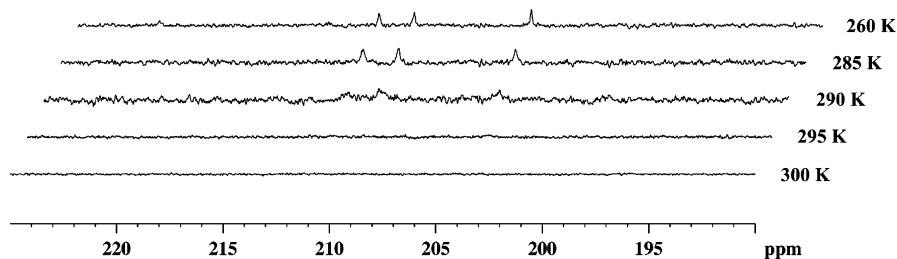


Table 1. Labeling Scheme, Hammett Values, and Infrared Spectroscopic Data for the Ligands and Complexes Prepared



R	Label	Hammett Value	$\nu(\text{CO}) / \text{cm}^{-1}$		
	<b>a</b>	0	2068	2009	1990
	<b>b</b>	-0.83	2061	2001	1982
	<b>c</b>	-0.27	2065	2005	1986
	<b>d</b>	0	2067	2008	1989
	<b>e</b>	0.23	2070	2011	1990
	<b>f</b>	0.39	2070	2011	1990
	<b>g</b>	0.54	2071	2013	1992
	<b>h</b>	0.12	2068	2009	1989
	<b>i</b>	0.43	2071	2013	1992
	<b>j</b>		2073	2016	1990
	<b>k</b>		2070	2012	1990
	<b>l</b>		2071	2013	1990
	<b>m</b>		2067	2008	1987
	<b>n</b>		2062	2001	1985



**Figure 3.** Variable-temperature  $^{13}\text{C}\{^1\text{H}\}$  NMR spectrum (M–CO) region of **2a**.

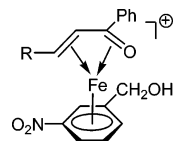


**Figure 4.** Structure of the proposed complexes formed in the 3-NOBA matrix.

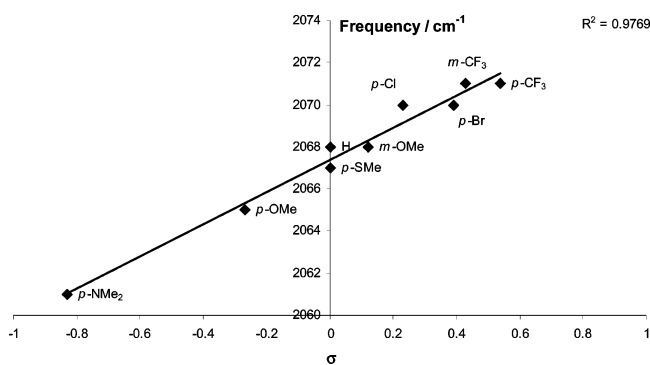


**Figure 5.** Plot of Hammett parameter versus infrared stretching frequency for band 1.

stretching modes in the iron(0) tricarbonyl group for the complexes. As can be seen from the Hammett plot<sup>25</sup> in Figure 5, there is a clear linear relationship between the Hammett values for the substituent positioned on the aromatic ring on the  $\beta$ -carbon and the frequency of the infrared bands due to the C–O stretch vibrations. As might be expected, substituents with net electron-withdrawing properties (such as  $-\text{CF}_3$ ) result in a band at higher frequency, whereas net electron-donating substituents (such as  $\text{NMe}_2$ ) result in a band at lower frequency. This phenomenon may simply be rationalized in terms of the amount of electron density available at the metal that may be donated into the antibonding orbitals of the carbon monoxide ligands, but it does not, however, provide any information as to whether the chalcone is primarily acting as a donor or acceptor ligand as, in both of these cases, the observed change in stretching frequencies would be predicted.

Considerable substituent effects are also observed in the NMR spectra of the complexes and ligands; indeed, in the free ligand a linear correlation has been observed between the resonance

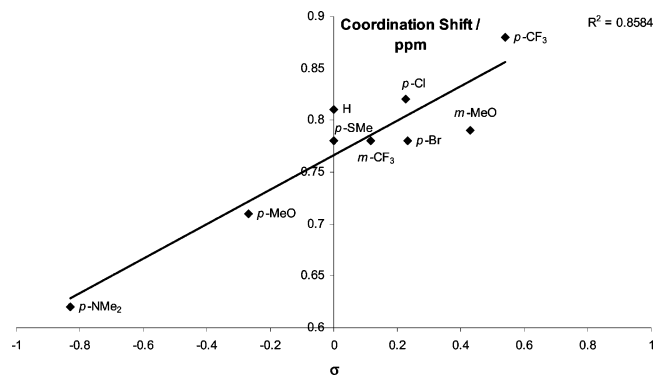


**Figure 6.** Plot of change in  $\text{H}_a$  signal on complexation versus  $\sigma$ .

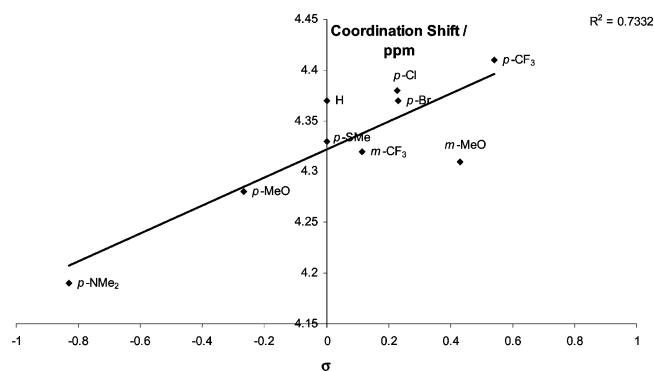


**Figure 7.** Plot of change in  $\text{H}_b$  signal on complexation versus  $\sigma$ .

for  $\text{C}_c$  and the electronic properties of suitable substituents.<sup>26</sup> In order, therefore, to gauge the effects of the substituent on the *coordinated* chalcone ligand, the coordination chemical shift (defined, in this instance, as  $\Delta\delta = \delta_{\text{free}} - \delta_{\text{coordinated}}$ ) was employed. This method ensures that any *intrinsic* effect on the chemical shift of a resonance due to a particular substituent is removed; hence the coordination shift will be diagnostic of the effect on metal–ligand interactions caused by different chalcone ligands. Plots of the coordination shift of  $\text{H}_a$ ,  $\text{H}_b$ ,  $\text{C}_B$ , and  $\text{C}_C$  are presented in Figures 6, 7, 8, and 9, respectively.

An examination of these plots illustrates that there is a linear relationship in all four cases between the coordination shift and the Hammett parameter, indicating that the electronic effect of the substituents on the chalcone does indeed play an important role in the bonding between the metal and this ligand. It is also evident from these data that the *largest coordination shifts are observed for the ligands that possess more electron-withdrawing substituents and smallest for those which are electron donating*. This in turn has the implication that chalcones with more electron-withdrawing substituents are coordinated more strongly to the iron. This trend is in keeping with studies reported by Knölker and co-workers, who have demonstrated that  $[\text{Fe}(\text{CO})_3-$

(20) Kruczynski, L.; Takats, J. *Inorg. Chem.* **1976**, *15*, 3140.

(21) In our hands, **2a** proved to be prone to thermal decomposition in solution. This prohibited comprehensive studies into the higher temperature regime of this exchange process.

(22) Gunther, H. *NMR Spectroscopy*, 2nd ed.; John Wiley and Sons: New York, 1995; p 344.

(23) Howell, J. A. S.; Dixon, D. T.; Kola, J. C. *J. Organomet. Chem.* **1984**, *266*, 69.

(24) (a) Knölker, H. J.; Baum, G.; Foitzik, N.; Goesmann, H.; Gonsler, P.; Jones, P. G.; Röttele, H. *Eur. J. Inorg. Chem.* **1998**, 993. (b) Knölker, H. J.; Goesmann, H.; Gonsler, P. *Tetrahedron Lett.* **1996**, *37*, 6543.

(25) Wiberg, K. *Physical Organic Chemistry*; John Wiley and Sons: New York, 1964; p 281.

(26) Ortega-Alfaro, M. C.; López-Cortés, J. G.; Toscano, R. A.; Alvarez-Toledano, C. *J. Braz. Chem. Soc.* **2005**, *16*, 362.

Table 2. Bond Lengths (Å) and Angles (deg) for the Structures of the Free Chalcones and Their Complexes<sup>a</sup>

	1i	1m	2a	2g	2i	2j	2k	2l
O <sub>1</sub> -C <sub>A</sub>	1.2279(14)	1.2268(12)	1.3115(19)	1.311(3)	1.3056(19)	1.3056(16)	1.310(2)	1.308(2)
C <sub>A</sub> -C <sub>B</sub>	1.4879(15)	1.4804(14)	1.429(2)	1.427(3)	1.424(2)	1.4275(18)	1.420(3)	1.425(3)
C <sub>B</sub> -C <sub>C</sub>	1.3392(15)	1.3408(14)	1.423(2)	1.428(3)	1.425(2)	1.4307(17)	1.425(3)	1.427(3)
Fe-O <sub>1</sub>			2.0153(12)	2.0201(17)	2.0132(12)	2.0099(10)	2.0114(13)	2.0156(14)
Fe-C <sub>A</sub>			2.0758(16)	2.083(2)	2.1026(16)	2.0929(13)	2.0978(17)	2.0847(19)
Fe-C <sub>B</sub>			2.0572(17)	2.070(2)	2.0673(16)	2.0681(14)	2.0695(18)	2.0654(19)
Fe-C <sub>C</sub>			2.1248(17)	2.118(2)	2.1138(17)	2.1156(13)	2.1206(18)	2.1048(19)
Fe-C <sub>D</sub>			1.8198(19)	1.819(3)	1.8348(18)	1.8240(15)	1.827(2)	1.821(2)
Fe-C <sub>E</sub>			1.8236(19)	1.833(3)	1.8180(18)	1.8306(14)	1.832(2)	1.833(2)
Fe-C <sub>F</sub>			1.776(2)	1.772(3)	1.7755(17)	1.7752(14)	1.768(2)	1.776(2)
C <sub>D</sub> -O <sub>2</sub>			1.133(2)	1.136(3)	1.134(2)	1.1327(18)	1.133(3)	1.136(3)
C <sub>E</sub> -O <sub>3</sub>			1.130(2)	1.132(3)	1.135(2)	1.1323(17)	1.130(3)	1.131(2)
C <sub>F</sub> -O <sub>4</sub>			1.142(2)	1.145(3)	1.137(2)	1.1393(17)	1.146(3)	1.142(2)
C <sub>F</sub> -Fe-O <sub>1</sub>			164.52(7)	162.00(9)	165.97(6)	166.22(5)	164.91(8)	163.63(7)
C <sub>E</sub> -Fe-C <sub>1</sub>			132.01(8)	133.56(11)	132.34(7)	134.60(5)	131.07(8)	135.46(8)
C <sub>E</sub> -Fe-C <sub>2</sub>			130.12(8)	132.96(10)	133.24(8)	135.40(6)	131.79(9)	134.94(8)
C <sub>D</sub> -Fe-C <sub>C</sub>			160.53(8)	164.17(10)	158.55(7)	160.82(6)	161.29(8)	160.49(8)
C <sub>D</sub> -Fe-O <sub>1</sub>			92.48(7)	93.55(9)	93.35(7)	92.50(5)	93.53(8)	92.63(8)
C <sub>F</sub> -Fe-C <sub>C</sub>			95.39(8)	95.14(10)	92.29(7)	95.96(6)	94.23(8)	94.01(8)
C <sub>D</sub> -Fe-C <sub>E</sub>			106.67(9)	100.50(11)	105.99(8)	101.36(6)	104.10(10)	102.63(9)
C <sub>E</sub> -Fe-C <sub>F</sub>			97.35(9)	99.38(12)	94.59(8)	94.04(6)	97.95(10)	95.36(9)
C <sub>C</sub> -Fe-C <sub>F</sub>			89.71(9)	88.26(11)	91.12(8)	90.15(6)	89.36(9)	90.76(9)

<sup>a</sup> The structure of **2a** contains four independent molecules in the asymmetric unit: the vast majority of the metrics for the independent molecules are statistically identical. For clarity, the data for only one of the molecules are presented.

{ $\eta^4$ -(R)<sub>2</sub>C=C-C=N(R')}] complexes exhibit dramatic substituent effects, which has enabled the complexes to be exploited as effective transfer agents of the "Fe(CO)<sub>3</sub>" unit to less reactive 1,3-dienes.<sup>27</sup> Furthermore, a study on the kinetics of the formation of iron tricarbonyl 1-azabuta-1,3-diene complexes from the corresponding tetracarbonyl species has demonstrated that the loss of the 1-azabuta-1,3-diene is slowest when the aryl group directly attached to the nitrogen contains an electron withdrawing group.<sup>28</sup>

An examination of the frontier molecular orbitals involved in the bonding between the ligand and the metal described in Figure 1 provides a framework for rationalizing these observations. The theoretical calculations by Calhorda and Vichi<sup>19</sup> using the extended Hückel method illustrate that the bonding between the metal and the ligand is dominated by donation from orbitals  $\pi_1$  and  $\pi_2$  to vacant metal-centered orbitals and donation from a full metal orbital to the vacant  $\pi_3$ -orbital on the ligand: donation to  $\pi_4$  is thought to be only a minor component. The fact that ligands containing electron-withdrawing groups, which are by definition the best electron acceptors, are more tightly bonded to the metal than those containing electron-donating substituents is consistent with a situation where the bonding between the iron(0) and the ligand is dominated by the donation from the metal into the vacant  $\pi_3$ -orbital. Further support for this interpretation is provided by the calculated orbital populations of the ligand-based orbitals  $\pi_1$ ,  $\pi_2$ ,  $\pi_3$ , and  $\pi_4$  in [Fe(CO)<sub>3</sub>( $\eta^4$ -PhCH=CH-C{Me})], which are 1.952, 1.919, 1.101, and 0.040, respectively.<sup>19</sup> This indicates that  $\pi_1$  and  $\pi_2$  exhibit only minor depopulation on coordination to the metal; in contrast,  $\pi_3$  becomes more than half-filled, indicating that the ligand is acting as a net acceptor of electrons. This description is consistent with the trends observed by NMR spectroscopy.

**d. X-ray Crystallography.** The structures of six chalcone complexes and two free ligands were determined by single-crystal X-ray diffraction. Selected bond lengths and angles for all of the structures are presented in Table 2, and the

experimental details of the structure determinations are listed in Table 3. The structure determinations of the two uncoordinated chalcones (**1i**, Figure 10; **1m**, Figure 11) illustrated that these species adopt the *s-cis* conformation in the solid state. The bond lengths with the C-C-C-O backbone exhibit a "short" O<sub>1</sub>-C<sub>A</sub>, "long" C<sub>A</sub>-C<sub>B</sub>, "short" C<sub>B</sub>-C<sub>C</sub> pattern. The six iron(0) complexes are also essentially isostructural. Representative complexes **2g** and **2l** are illustrated in Figures 12 and 13. The chalcone ligands exhibit the expected *s-cis* (single-bond geometry connecting the enone) conformation, and the bond lengths within the C-C-C-O framework exhibit the changes that are predicted on the basis of the bonding models described above; namely, the O<sub>1</sub>-C<sub>A</sub> and C<sub>B</sub>-C<sub>C</sub> bonds show significant lengthening on coordination to the metal, whereas C<sub>A</sub>-C<sub>B</sub> exhibits shortening, compared to the free ligand.<sup>26,29-32</sup> An examination of the bond angles around the iron indicates that the complexes are best considered to be six-coordinate octahedral species with three coordination sites occupied by the carbonyl ligands, with the remaining position occupied by O<sub>1</sub>, C<sub>C</sub>, and the center of the C<sub>A</sub>-C<sub>B</sub> bond. The mean bond angles around the iron for all six complexes are shown in Figure 14. The most marked deviations from an idealized octahedral geometry are the bond angles C<sub>D</sub>-Fe-C<sub>E</sub> (mean 103.54°) and also the angle subtended by the center of the C<sub>A</sub>-C<sub>B</sub> bond, the iron, and C<sub>E</sub> (typically 134°).

Our attempts to draw correlations between the metrics within the X-ray structures and the electronic properties of the attached substituents on chalcone have been frustrated by the fact that we have, to date, not been able to grow single crystals of all of the complexes and ligands that have been prepared. A quantitative analysis of the substituent effects of the bond lengths within the coordinated ligands may be made only when a comparison is made between free and coordinated ligands possessing the same functional group so that, in the same manner as the

(29) Vichi, E. J. S.; Raithby P. R.; McPartlin, M. *J. Organomet. Chem.* **1983**, 256, 111.

(30) Marcuzzi, A.; Linden A.; von Phillipsborn, W. *Helv. Chim. Acta* **1993**, 76, 976.

(31) Bender, B.; Koller, M.; Linden, A.; Marcuzzi A.; von Phillipsborn, W. *Organometallics* **1992**, 11, 4268.

(32) Sacerdoti, M.; Betolasi, V.; Gilli, G. *Acta Crystallogr. Sect. B* **1980**, 36, 1061.

(27) (a) Knölker, H.-J.; Gonsor, P. *Synlett* **1992**, 517. (b) Knölker, H.-J.; Gonsor, P.; Jones, P. G. *Synlett* **1994**, 405. (c) Knölker, H.-J.; Baum, E.; Gonsor, P.; Röhde, G.; Röttele, H. *Organometallics* **1998**, 17, 3916.

(28) Bellachioma, G.; Cardaci, G. *J. Chem. Soc., Dalton Trans.* **1977**, 909.

Table 3. Crystal Data and Refinement Information for the X-ray Structures

	1i	1m	2a	2g	2i	2j	2k	2l
empirical formula	C <sub>16</sub> H <sub>11</sub> F <sub>3</sub> O	C <sub>18</sub> H <sub>18</sub> O <sub>4</sub>	C <sub>18</sub> H <sub>12</sub> FeO <sub>4</sub>	C <sub>19</sub> H <sub>11</sub> F <sub>3</sub> FeO <sub>4</sub>	C <sub>19</sub> H <sub>11</sub> F <sub>3</sub> FeO <sub>4</sub>	C <sub>19</sub> H <sub>11</sub> F <sub>3</sub> FeO <sub>4</sub>	C <sub>18</sub> H <sub>11</sub> FFeO <sub>4</sub>	C <sub>18</sub> H <sub>11</sub> ClFeO <sub>4</sub>
fw	276.25	298.32	348.13	416.13	416.13	416.13	366.12	382.57
temp/K	100(2)	100(2) K	100(2) K	100(2) K	100(2) K	100(2) K	100(2) K	100(2) K
wavelength/Å	0.71073	0.71073 Å	0.71073 Å	0.71073 Å	0.71073 Å	0.71073 Å	0.71073 Å	0.71073 Å
cryst syst	triclinic	monoclinic	orthorhombic	monoclinic	triclinic	monoclinic	orthorhombic	monoclinic
space group	<i>P</i> $\bar{1}$	<i>P</i> 2(1)/ <i>c</i>	<i>Pca</i> 2(1)	<i>P</i> 2(1)/ <i>c</i>	<i>P</i> $\bar{1}$	<i>P</i> 2(1)/ <i>c</i>	<i>Pccn</i>	<i>P</i> 2(1)/ <i>c</i>
<i>a</i> /Å	5.8276(6)	13.5188(8)	26.628(4)	10.8542(18)	8.0365(9)	11.428(2)	12.0533(13)	11.2496(11)
<i>b</i> /Å	7.3421(8)	7.8075(5)	11.3210(16)	16.111(3)	9.4564(11)	16.292(3)	22.984(3)	15.2045(16)
<i>c</i> /Å	14.8654(15)	14.9709(9)	20.637(3)	10.4171(17)	12.2370(14)	9.2583(17)	11.3950(12)	9.4967(10)
$\alpha$ /deg	95.448(2)	90	90	90	110.728(2)	90	90	90
$\beta$ /deg	94.829(2)	109.7970(10)	90°	111.817(3)	92.247(2)	103.249(4)	90	102.491(2)
$\gamma$ /deg	92.512(2)	90	90	90	100.016(2)	90	90	90
volume/Å <sup>3</sup>	630.06(11)	1486.76(16)	6221.0(15)	1691.2(5)	851.37(17)	1677.9(5)	3156.8(6)	1585.9(3)
<i>Z</i>	2	4	16	4	2	4	8	4
density (calcd)/Mg/m <sup>3</sup>	1.456	1.333	1.487	1.634	1.623	1.647	1.541	1.602
absorp coeff/mm <sup>-1</sup>	0.120	0.094	0.986	0.946	0.940	0.954	0.985	1.138
<i>F</i> (000)	284	632	2848	840	420	840	1488	776
cryst size/mm <sup>3</sup>	0.29 × 0.22 × 0.18	0.27 × 0.17 × 0.13	0.24 × 0.17 × 0.17	0.25 × 0.18 × 0.07	0.32 × 0.16 × 0.06	0.27 × 0.10 × 0.08	0.40 × 0.06 × 0.06	0.13 × 0.07 × 0.05
$\theta$ range for data collection/deg	2.76 to 30.02	1.60 to 29.99°	1.53 to 30.03°	2.02 to 30.01°	1.79 to 30.01°	1.83 to 30.05°	1.77 to 30.02°	1.85 to 30.05°
index ranges	-8 ≤ <i>h</i> ≤ 8, -10 ≤ <i>k</i> ≤ 10, -20 ≤ <i>l</i> ≤ 20	-19 ≤ <i>h</i> ≤ 19, -10 ≤ <i>k</i> ≤ 10, -20 ≤ <i>l</i> ≤ 20	-36 ≤ <i>h</i> ≤ 37, -15 ≤ <i>k</i> ≤ 15, -28 ≤ <i>l</i> ≤ 28	-15 ≤ <i>h</i> ≤ 15, -22 ≤ <i>k</i> ≤ 22, -14 ≤ <i>l</i> ≤ 14	-11 ≤ <i>h</i> ≤ 11, -13 ≤ <i>k</i> ≤ 13, -16 ≤ <i>l</i> ≤ 17	-15 ≤ <i>h</i> ≤ 15, -22 ≤ <i>k</i> ≤ 22, -12 ≤ <i>l</i> ≤ 12	-16 ≤ <i>h</i> ≤ 16, -32 ≤ <i>k</i> ≤ 31, -15 ≤ <i>l</i> ≤ 15	-15 ≤ <i>h</i> ≤ 15, -21 ≤ <i>k</i> ≤ 21, -13 ≤ <i>l</i> ≤ 13
no. of reflns collected	6945	15 963	68 566	18 270	9279	18 656	33 390	17 600
no. of indep reflns	3478	4269	17 701	4853	4706	4781	4590	4578
completeness to $\theta$	[ <i>R</i> (int) = 0.0122] 94.7% (30.02°)	[ <i>R</i> (int) = 0.0214] 98.8% (29.9°)	[ <i>R</i> (int) = 0.0289] 99.5% (30.03°)	[ <i>R</i> (int) = 0.0459] 98.1% (30.01°)	[ <i>R</i> (int) = 0.0213] 94.5% (30.01°)	[ <i>R</i> (int) = 0.0221] 97.3% (30.05°)	[ <i>R</i> (int) = 0.0448] 99.4% (30.02°)	[ <i>R</i> (int) = 0.0397] 98.4% (30.05°)
absorp corr				semiempirical from equivalents				
max. and min. transmn	0.980 and 0.815	1.000 and 0.815	1.000 and 0.917	0.940 and 0.726	0.940 and 0.870	1.000 and 0.763	1.000 and 0.881	0.940 and 0.832
refinement method				full-matrix least-squares on <i>F</i> <sup>2</sup>				
no. of data/restraints/params	3478/0/225	4269/0/202	17 701/1/862	4853/0/244	4706/0/252	4781/0/288	4590/0/217	4578/0/261
goodness-of-fit on <i>F</i> <sup>2</sup>	1.019	1.026	1.036	1.048	1.028	1.020	1.029	1.040
final <i>R</i> indices [ <i>I</i> > 2 $\sigma$ ( <i>I</i> )]	<i>R</i> 1 = 0.0451, w <i>R</i> 2 = 0.1225	<i>R</i> 1 = 0.0439, w <i>R</i> 2 = 0.1145	<i>R</i> 1 = 0.0307, w <i>R</i> 2 = 0.0720	<i>R</i> 1 = 0.0473, w <i>R</i> 2 = 0.1179	<i>R</i> 1 = 0.0336, w <i>R</i> 2 = 0.0775	<i>R</i> 1 = 0.0296, w <i>R</i> 2 = 0.0746	<i>R</i> 1 = 0.0417, w <i>R</i> 2 = 0.0963	<i>R</i> 1 = 0.0407, w <i>R</i> 2 = 0.0832
<i>R</i> indices (all data)	<i>R</i> 1 = 0.0495, w <i>R</i> 2 = 0.1262	<i>R</i> 1 = 0.0508, w <i>R</i> 2 = 0.1195	<i>R</i> 1 = 0.0351, w <i>R</i> 2 = 0.0741	<i>R</i> 1 = 0.0695, w <i>R</i> 2 = 0.1296	<i>R</i> 1 = 0.0476, w <i>R</i> 2 = 0.0833	<i>R</i> 1 = 0.0346, w <i>R</i> 2 = 0.0773	<i>R</i> 1 = 0.0638, w <i>R</i> 2 = 0.1063	<i>R</i> 1 = 0.0560, w <i>R</i> 2 = 0.0882
largest diff peak and hole/e Å <sup>-3</sup>	0.551 and -0.337	0.525 and -0.176	0.565 and -0.207	1.004 and -0.560	0.541 and -0.400	0.449 and -0.229	0.952 and -0.491	0.602 and -0.292

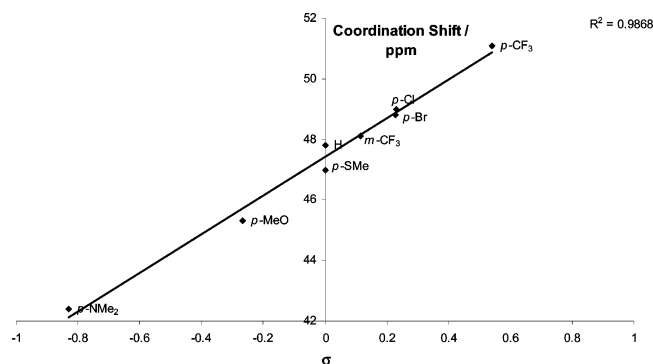


Figure 8. Hammett plot of the coordination shift of  $C_B$ .

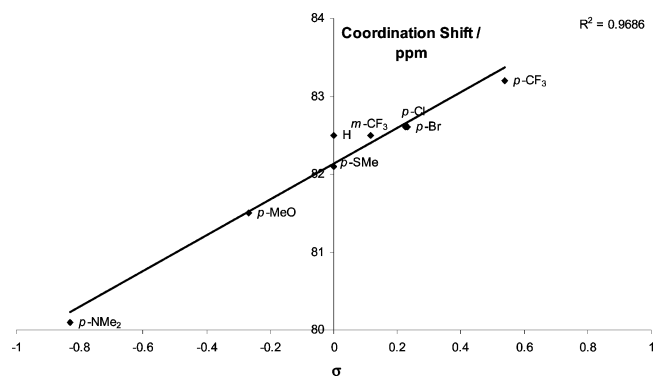


Figure 9. Hammett plot of the coordination shift of  $C_C$ .

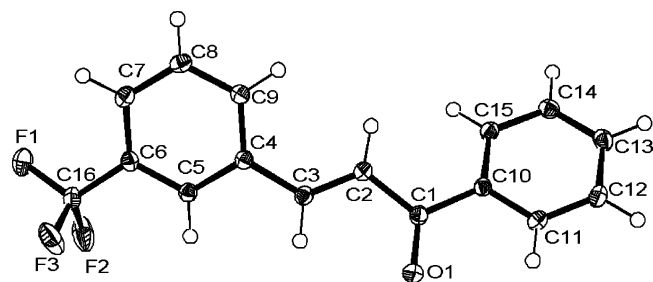


Figure 10. ORTEP representation of the structure of compound **1i**. Thermal ellipsoids are shown at the 50% probability level.

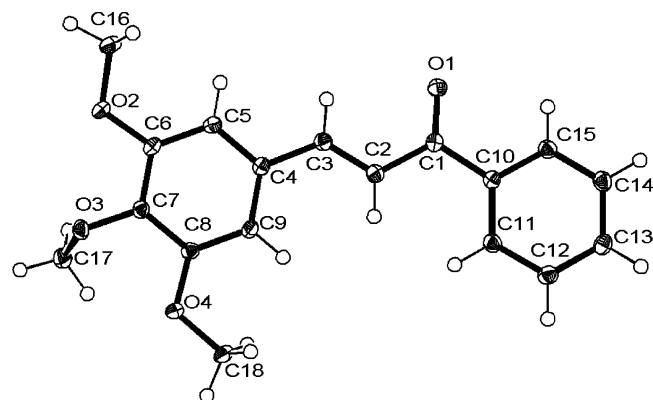


Figure 11. ORTEP representation of the structure of compound **1m**. Thermal ellipsoids are shown at the 50% probability level.

treatment of the NMR spectra of these compounds, an evaluation of the change in bond length on coordination may be made. With this in mind, it was anticipated that the bond lengths within the metal carbonyl ligands might be used to probe the changes in the electronic environment of the iron induced by the substituents on the chalcone ligand.

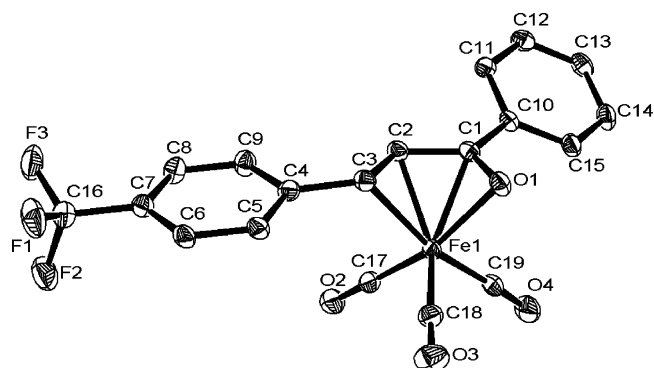


Figure 12. ORTEP representation of the structure of compound **2g**. Thermal ellipsoids are shown at the 50% probability level; hydrogen atoms are omitted for clarity.

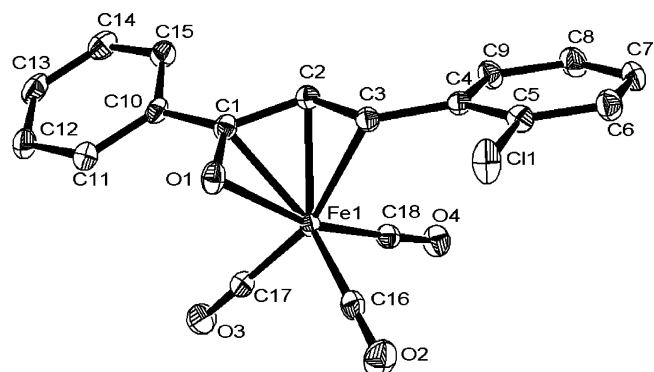


Figure 13. ORTEP representation of the structure of compound **2l**. Thermal ellipsoids are shown at the 50% probability level; hydrogen atoms are omitted for clarity.

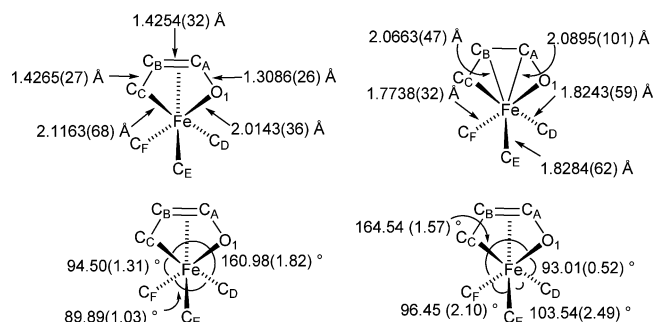
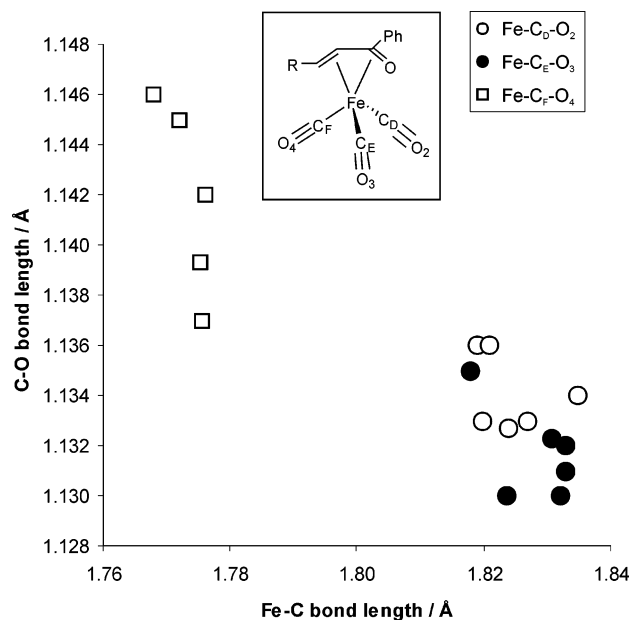


Figure 14. Mean bond angles around the iron atom: standard deviation from the mean shown in parentheses.

An examination of the Fe–C bond lengths within the carbonyl ligands revealed that, in all cases, the Fe– $C_F$  bond was considerably shorter (mean  $1.7738$  Å) than both Fe– $C_E$  (mean  $1.8284$  Å) and Fe– $C_D$  (mean  $1.8243$  Å). This may be simply rationalized on the basis that  $C_F$  is in a position essentially *trans* to  $O_1$ , which is predicted to be the best donor group,<sup>6,19</sup> and  $C_D$  is *trans* to  $C_C$ , the best acceptor. A comparison of the Fe–C and C–O bonds lengths (Figure 11) shows the expected correlation between shorter Fe–C bonds with longer C–O bonds and further illustrates the difference between the bonding situation involving  $C_F$  and the other two ligands.<sup>33</sup> The three carbonyl ligands in these complexes fall into region 2 under the classification system of Hocking and Hambley,<sup>33</sup> in which  $\sigma$ - and  $\pi$ -effects are in balance.

Even though the structures are of a high quality (as measured by estimated standard deviations in bond lengths and angles





**Figure 15.** Plot of C–O versus M–C bond lengths for the carbonyl ligands in the chalcone complexes

and  $R_1$  and  $wR_2$  parameters), the precision of the X-ray diffraction experiments does not allow for any insight to be gained into the effects of the substituted chalcone on the metal–ligand bonding. The differences in the bond lengths between the iron and the carbon atoms of the carbonyl group (and indeed within the chalcone ligands themselves) in the majority of the complexes are not of any statistical significance. The changes induced by the different aryl substituents are too subtle to be evaluated by this method; furthermore, the effect of crystal-packing forces on the structural metrics may not be easily deconvoluted. As has been commented previously,<sup>6</sup> it is clear that, even with high-quality crystal structures acquired at low temperature, NMR spectroscopy is a far more sensitive technique for probing subtle changes in the electronic structure of these complexes.

**e. Conclusions.** A valuable library of iron(0) tricarbonyl complexes has been prepared by reaction of the chalcone ligands with  $[\text{Fe}_2(\text{CO})_9]$  in diethyl ether. From a detailed analysis of the IR and NMR spectroscopic data of these species it is clear that the substituents on the chalcone significantly affect the resulting metal–ligand interactions and that linear relationships exist between the well-known Hammett parameters and these spectroscopic properties. Although the trends within the IR spectroscopic data for the metal carbonyl ligands are more predictable, with more electron-withdrawing substituents resulting in less back-bonding to the metal carbonyl ligands and *vice versa*, the NMR spectra have allowed us to deconvolute the relative importance of the donor/acceptor interactions between the ligand and the metal. Our results demonstrate that the chalcone ligand binds more strongly to the metal when electron-withdrawing groups are present on the chalcone. This is in line with a previous theoretical study, which predicted that  $\alpha,\beta$ -unsaturated enone ligands act as “net” electron-withdrawing groups. In keeping with studies reported by Knölker and co-workers<sup>24,27</sup> on ligand lability in  $(\eta^4\text{-azabutadiene})\text{Fe}(\text{CO})_3$  complexes, the results presented in this study predict that complexes containing more electron-rich chalcone ligands ought to be more effective transfer agents of the “ $\text{Fe}(\text{CO})_3$ ” group.

## Experimental Section

**General Details.** THF and  $\text{Et}_2\text{O}$  were dried over sodium-benzophenone ketyl (distilled prior to use) when necessary. TLC analysis was performed on Merck 5554 aluminum-backed silica gel plates, and compounds were visualized by ultraviolet light (254 nm). The relative proportion of solvents in mixed chromatography solvents refers to the volume/volume ratio. Infrared spectra were recorded on a ATI Mattson Genesis FT-IR. Mass spectrometry was carried out using a Fisons Analytical (VG) Autospec instrument. High-resolution masses are within 5 ppm of theoretical values. NMR spectra were recorded in the deuterated solvent indicated on either a JEOL ECX400 spectrometer (operating frequencies  $^1\text{H}$  400.13 MHz  $^{13}\text{C}$  100.5 MHz) or a Bruker AV500 spectrometer (operating frequencies  $^1\text{H}$  500.13,  $^{13}\text{C}$  125.78 MHz). Chemical shifts are reported in parts per million ( $\delta$ ) downfield from an internal tetramethylsilane reference. Coupling constants ( $J$  values) are reported in hertz (Hz), and spin multiplicities are indicated by the following symbols: s (singlet), d (doublet), t (triplet), q (quartet), qn (quintet), sx (sextet), m (multiplet), br (broad). **1a** and **1e** were purchased from Aldrich and used as supplied.

**General Procedure for the Synthesis of the Substituted Chalcones.** To an aqueous alcoholic solution (1.5 mL per mmol; ratio  $\text{EtOH}:\text{H}_2\text{O}$  of 1:2) of NaOH (1.25 equiv) was added acetophenone (1 equiv). The reaction mixture was cooled in ice, and the substituted benzaldehyde (1 equiv) was added dropwise. The reaction mixture was stirred at room temperature for 16 h. The solid formed was removed by filtration, washed with  $\text{H}_2\text{O}$ , and recrystallized from hot  $\text{EtOH}$ . If precipitation did not occur, the reaction mixture was extracted with  $\text{Et}_2\text{O}$  ( $3 \times 50$  mL). The combined  $\text{Et}_2\text{O}$  layers were washed with brine, dried with  $\text{MgSO}_4$ , and concentrated *in vacuo* to yield the desired products as colorless to pale yellow crystalline solids, with the exception of orange **1b**.

**(E)-3-(4-Dimethylaminophenyl)-1-phenyl-2-propen-1-one, 1b.** Yield: 42%.  $\delta_{\text{H}}$  (500 MHz,  $\text{CDCl}_3$ ): 3.04 (s, 6H), 6.69 (d, 2H,  $J = 8.87$  Hz), 7.34 (d, 1H,  $J = 15.49$  Hz), 7.48 (t, 2H,  $J = 7.43$  Hz), 7.53–7.57 (m, 3H), 7.78 (d, 1H,  $J = 15.50$  Hz), 7.99–8.02 (m, 2H).  $\delta_{\text{C}}$  (125 MHz,  $\text{CDCl}_3$ ): 40.1 ( $\text{CH}_3$ ), 111.8 (CH), 116.9 (CH), 122.6 ( $4^\circ$ ), 128.3 (CH), 128.4 (CH), 130.4 (CH), 132.2 (CH), 139.0 ( $4^\circ$ ), 145.8 (CH), 152.0 ( $4^\circ$ ), 190.7 ( $4^\circ$ ).  $m/z$  (CI): 207 (M–NMe<sub>2</sub>, 12%), 252 (MH<sup>+</sup>, 100%). IR ( $\text{CH}_2\text{Cl}_2$ ): 1712, 1652, 1570, 1527, 1365, 1344, 1227, 1171.

**(E)-3-(4-Methoxyphenyl)-1-phenyl-2-propen-1-one, 1c.** Yield: 68%.  $\delta_{\text{H}}$  (500 MHz,  $\text{CDCl}_3$ ): 3.85 (s, 3H), 6.94 (d, 2H,  $J = 8.7$  Hz), 7.41 (d, 1H,  $J = 15.64$  Hz), 7.50 (t, 2H,  $J = 7.5$  Hz), 7.56–7.61 (m, 3H), 7.79 (d, 1H,  $J = 15.64$  Hz), 8.01 (d, 2H,  $J = 7.3$  Hz).  $\delta_{\text{C}}$  (125 MHz,  $\text{CDCl}_3$ ): 55.4 ( $\text{CH}_3$ ), 114.4 (CH), 119.7 (CH), 127.6 ( $4^\circ$ ), 128.4 (CH), 128.5 (CH), 130.2 (CH), 132.5 (CH), 138.5 ( $4^\circ$ ), 144.7 (CH), 161.6 ( $4^\circ$ ), 190.6 ( $4^\circ$ ).  $m/z$  (CI): 239 (MH<sup>+</sup>, 100%). IR ( $\text{CH}_2\text{Cl}_2$ ): 1661, 1595, 1573, 1511, 1292, 1250, 1215, 1172.

**(E)-3-(4-Methylthiophenyl)-1-phenyl-2-propen-1-one, 1d.** Yield: 72%.  $\delta_{\text{H}}$  (500 MHz,  $\text{CDCl}_3$ ): 2.52 (s, 3H), 7.26 (d, 2H,  $J = 8.39$  Hz), 7.46–7.52 (m, 3H (contains d, 7.49 ppm, 1H,  $J = 15.50$  Hz)), 7.54–7.60 (m, 3H), 7.77 (d, 1H,  $J = 15.67$  Hz), 7.00–8.03 (m, 2H).  $\delta_{\text{C}}$  (125 MHz,  $\text{CDCl}_3$ ): 15.1 ( $\text{CH}_3$ ), 121.0 (CH), 126.0 (CH), 128.4 (CH), 128.6 (CH), 128.8 (CH), 131.4 ( $4^\circ$ ), 132.6 (CH), 138.3 ( $4^\circ$ ), 142.4 ( $4^\circ$ ), 144.3 (CH), 190.4 ( $4^\circ$ ).  $m/z$  (CI): 207 (M – SMe, 14%), 255 (MH<sup>+</sup>, 100%). IR ( $\text{CH}_2\text{Cl}_2$ ): 1711, 1663, 1603, 1590, 1362, 1220.

**(E)-3-(4-Bromophenyl)-1-phenyl-2-propen-1-one, 1f.** Yield: 68%.  $\delta_{\text{H}}$  (500 MHz,  $\text{CDCl}_3$ ): 7.50–7.61 (m, 8H (overlaps d, 7.43 ppm, 1H,  $J = 15.7$  Hz)), 7.72 (d, 1H,  $J = 15.72$  Hz), 7.99–8.04 (m, 2H).  $\delta_{\text{C}}$  (125 MHz,  $\text{CDCl}_3$ ): 122.6 (CH), 124.8 ( $4^\circ$ ), 128.5 (CH), 128.7 (CH), 129.8 (CH), 132.2 (CH), 132.9 (CH), 133.8 ( $4^\circ$ ), 138.0 ( $4^\circ$ ), 143.3 (CH), 190.2 ( $4^\circ$ ).  $m/z$  (CI): 287/289 ( $\text{Br}^{79}/\text{Br}^{81}$  M<sup>+</sup>, 100%). IR ( $\text{CH}_2\text{Cl}_2$ ): 1665, 1607, 1587, 1487, 1330, 1215.

**(E)-3-(4-Trifluoromethylphenyl)-1-phenyl-2-propen-1-one, 1g.** Yield: 75%.  $\delta_{\text{H}}$  (500 MHz,  $\text{CDCl}_3$ ): 7.48–7.56 (m, 2H), 7.57–7.64 (m, 2H (containing d, 7.60 ppm, 1H,  $J = 15.72$  Hz)), 7.68 (d, 2H,  $J = 8.24$  Hz), 7.74 (d, 2H,  $J = 8.24$  Hz), 7.81 (d, 1H,  $J = 15.76$  Hz), 8.02–8.05 (m, 2H).  $\delta_{\text{C}}$  (125 MHz,  $\text{CDCl}_3$ ): 123.8 (4°), q,  $J = 273$  Hz), 124.3 (CH), 125.8 (CH, q, 3.7 Hz), 128.5 (CH), 128.5 (CH), 128.7 (CH), 131.9 (4°, q,  $J = 32.6$  Hz), 133.1 (CH), 137.8 (4°), 138.3 (4°), 142.7 (CH), 190.0 (4°);  $m/z$  (CI) 207 (M –  $\text{CF}_3$ , 33%), 277 (MH<sup>+</sup>, 100%), IR ( $\text{CH}_2\text{Cl}_2$ ) 1668, 1610, 1324, 1287, 1216, 1171, 1129, 1068, 1015.

**(E)-3-(3-Methoxyphenyl)-1-phenyl-2-propen-1-one, 1h.** Yield: 50%.  $\delta_{\text{H}}$  (500 MHz,  $\text{CDCl}_3$ ): 3.86 (s, 3H), 6.97 (dd, 1H,  $J = 7.97$ , 2.16 Hz), 7.16 (s, 1H), 7.24 (d, 1H,  $J = 6.65$  Hz), 7.34 (t, 1H,  $J = 7.90$  Hz), 7.48–7.54 (m, 3H (contains d, 1H, 7.51 ppm,  $J = 15.63$  Hz), 7.59 (t, 1H,  $J = 7.36$  Hz), 7.77 (d, 1H,  $J = 15.71$  Hz), 8.00–8.04 (m, 2H).  $\delta_{\text{C}}$  (125 MHz,  $\text{CDCl}_3$ ): 55.3 (CH<sub>3</sub>), 113.4 (CH), 116.3 (CH), 121.1 (CH), 122.4 (CH), 128.5 (CH), 128.6 (CH), 129.9 (CH), 132.8 (CH), 136.2 (4°), 138.2 (4°), 144.7 (CH), 159.9 (4°), 190.5 (4°).  $m/z$  (CI): 207 (M – Ome, 42%), 239 (MH<sup>+</sup>, 100%). IR ( $\text{CH}_2\text{Cl}_2$ ): 1664, 1606, 1579, 1487, 1448, 1315, 1257.

**(E)-3-(3-Trifluoromethylphenyl)-1-phenyl-2-propen-1-one, 1i.** Yield: 44%.  $\delta_{\text{H}}$  (500 MHz,  $\text{CDCl}_3$ ): 7.40–7.61 (m, 6H, (contains d, 1H, 7.50 ppm,  $J = 15.87$  Hz)), 7.68–7.76 (m, 2H (contains d, 1H, 7.73 ppm,  $J = 15.82$  Hz)), 7.80 (s, 1H), 7.95 (d, 2H,  $J = 7.36$  Hz).  $\delta_{\text{C}}$  (125 MHz,  $\text{CDCl}_3$ ): 123.7 (CH), 123.8 (4°, q,  $J = 274$  Hz), 124.7 (CH, q,  $J = 4.0$  Hz), 126.8 (CH, q,  $J = 4.2$  Hz), 128.5 (CH), 128.7 (CH), 129.5 (CH), 131.5 (4°, q,  $J = 33$  Hz), 131.6 (4°), 133.3 (CH), 135.6 (CH), 137.8 (CH), 142.8 (4°), 190.2 (4°);  $m/z$  (CI) 277 (MH<sup>+</sup>, 100%), 294 (MNH<sub>4</sub><sup>+</sup>, 10%), IR ( $\text{CH}_2\text{Cl}_2$ ) 1667, 1610, 1336, 1214, 1169, 1131.

**(E)-3-(2-Trifluoromethylphenyl)-1-phenyl-2-propen-1-one, 1j.** Yield: 75%.  $\delta_{\text{H}}$  (500 MHz,  $\text{CDCl}_3$ ): 7.42 (d, 1H,  $J = 15.60$  Hz), 7.47–7.55 (m, 3H), 7.58–7.64 (m, 2H), 7.73 (d, 1H,  $J = 7.82$  Hz), 7.83 (d, 1H,  $J = 7.80$  Hz), 8.00–8.03 (m, 2H), 8.13 (dd, 1H,  $J = 15.62$ , 1.97 Hz).  $\delta_{\text{C}}$  (125 MHz,  $\text{CDCl}_3$ ): 123.9 (4°, q,  $J = 274$  Hz), 126.2 (CH, q,  $J = 5.6$  Hz), 126.6 (CH), 127.9 (CH), 128.7 (CH), 129.2 (4°, q,  $J = 30.4$  Hz), 129.7 (CH), 131.0 (CH), 132.1 (CH), 133.0 (CH), 134.0 (4°), 137.6 (4°), 140.2 (CH), 190.3 (4°);  $m/z$  (CI) 207 (M –  $\text{CF}_3$ , 10%), 277 (MH<sup>+</sup>, 100%), 294 (MNH<sub>4</sub><sup>+</sup>, 75%) IR ( $\text{CH}_2\text{Cl}_2$ ) 1668, 1648, 1612, 1577, 1314, 1291, 1217, 1164, 1128.

**(E)-3-(2-Fluorophenyl)-1-phenyl-2-propen-1-one, 1k.** Yield: 67%.  $\delta_{\text{H}}$  (500 MHz,  $\text{CDCl}_3$ ): 7.13 (dd, 1H,  $J = 10.32$ , 8.80 Hz), 7.20 (t, 1H,  $J = 7.54$  Hz), 7.36–7.41 (m, 1H), 7.51 (t, 2H,  $J = 7.58$  Hz), 7.59 (t, 1H,  $J = 7.36$  Hz), 7.64–7.67 (m, 2H (contains d, 7.65 ppm, 1H,  $J = 15.88$  Hz), 7.91 (d, 1H,  $J = 15.93$  Hz), 8.01–8.05 (2H, m).  $\delta_{\text{C}}$  (125 MHz,  $\text{CDCl}_3$ ): 116.2 (CH, d,  $J = 22.0$  Hz), 123.0 (4°, d,  $J = 11.5$  Hz), 124.5 (CH, d,  $J = 3.6$  Hz), 124.6 (CH, d,  $J = 7.2$  Hz), 128.5 (CH), 128.6 (CH), 129.8 (CH, d,  $J = 2.9$  Hz), 131.8 (CH, d,  $J = 8.8$  Hz), 132.9 (CH), 137.5 (CH, d,  $J = 1.9$  Hz), 138.0 (4°), 161.7 (4°, d,  $J = 254$  Hz), 190.5 (4°);  $m/z$  (CI) 227 (MH<sup>+</sup>, 100%); IR ( $\text{CH}_2\text{Cl}_2$ ) 1667, 1607, 1577, 1486, 1457, 1332, 1214.

**(E)-3-(2-Chlorophenyl)-1-phenyl-2-propen-1-one, 1l.** Yield: 71%.  $\delta_{\text{H}}$  (500 MHz,  $\text{CDCl}_3$ ): 7.27–7.36 (m, 2H), 7.41–7.52 (m, 4H (overlaps d, 7.47 ppm, 1H,  $J = 15.78$  Hz), 7.58 (t, 1H,  $J = 7.37$  Hz) 7.71–7.75 (m, 1H), 7.00–8.02 (m, 2H), 8.16 (d, 1H,  $J = 15.79$  Hz).  $\delta_{\text{C}}$  (125 MHz,  $\text{CDCl}_3$ ): 124.8 (CH), 127.1 (CH), 127.8 (CH), 128.6 (CH), 128.6 (CH), 130.2 (CH), 131.1 (CH), 132.9 (CH), 133.3 (4°), 135.5 (4°), 137.9 (4°), 140.6 (CH), 190.4 (4°).  $m/z$  (CI): 207 (M – Cl, 10%), 243/245 (Cl<sup>35</sup>/Cl<sup>37</sup> MH<sup>+</sup>, 100%), 260/262 (Cl<sup>35</sup>/Cl<sup>37</sup> MNH<sub>4</sub><sup>+</sup>, 5%). IR ( $\text{CH}_2\text{Cl}_2$ ): 1665, 1607, 1469, 1446, 1331, 1315, 1215.

**(E)-3-(3,4,5-Trimethoxyphenyl)-1-phenyl-2-propen-1-one, 1m.** Yield: 81%.  $\delta_{\text{H}}$  (400 MHz,  $\text{CDCl}_3$ ): 3.90 (3H, s), 3.92 (6H, s), 6.86 (2H, s), 7.40 (1H, d,  $J = 15.57$  Hz), 7.49–7.53 (2H, m), 7.57–

7.61 (1H, m), 7.72 (1H, d,  $J = 15.58$  Hz), 8.00–8.02 (2H, m);  $\delta_{\text{C}}$  (100.5 MHz,  $\text{CDCl}_3$ ): 56.2 (CH<sub>3</sub>), 61.0 (CH<sub>3</sub>), 105.5 (CH), 121.4 (CH), 128.4 (CH), 128.6 (CH), 130.3 (4°), 132.7 (CH), 138.2 (4°), 140.3 (4°), 145.0 (CH), 153.4 (4°), 190.6 (4°).  $m/z$  (CI): 299 (MH<sup>+</sup>, 100%). IR ( $\text{CH}_2\text{Cl}_2$ ): 1664, 1605, 1580, 1503, 1464, 1417, 1320, 1281, 1243, 1212, 1129.

**(E)-3-(2,4,6-Trimethylphenyl)-1-phenyl-2-propen-1-one, 1n.** Yield: 12%.  $\delta_{\text{H}}$  (500 MHz,  $\text{CDCl}_3$ ): 2.31 (s, 3H), 2.40 (s, 6H), 6.93 (s, 2H), 7.17 (d, 1H,  $J = 16.04$  Hz), 7.50 (t, 2H,  $J = 7.60$  Hz), 7.58–7.60 (m, 2H), 7.96–8.02 (m, 3H (containing d, 7.98 ppm, 1H,  $J = 15.74$  Hz)).  $\delta_{\text{C}}$  (125 MHz,  $\text{CDCl}_3$ ): 21.1 (CH<sub>3</sub>), 21.2 (CH<sub>3</sub>), 127.3 (CH), 128.5 (CH), 128.6 (CH), 129.3 (CH), 131.6 (4°), 132.7 (CH), 137.1 (4°), 138.2 (4°), 138.5 (4°), 143.3 (CH), 190.5 (4°).  $m/z$  (CI): 251 (MH<sup>+</sup>, 100%). IR ( $\text{CH}_2\text{Cl}_2$ ): 1665, 1605, 1449, 1327, 1308, 1216, 1015.

**General Procedure for the Complexation of Chalcones with Fe<sub>2</sub>(CO)<sub>9</sub>.** To a dried Schlenk tube under N<sub>2</sub> were added Fe<sub>2</sub>(CO)<sub>9</sub> (2 equiv) and the chalcone (1 equiv). Diethyl ether (12 mL per mmol) was added and the mixture heated at reflux for 16 h. The solution was diluted with 5 mL of Et<sub>2</sub>O and filtered through neutral alumina. Purification by column chromatography using hexane/Et<sub>2</sub>O (9:1, v/v) gave the expected chalcone complex.

$\eta^4$ -((E)-1,3-Diphenyl-2-propen-1-one)-tricarbonyliron(0), 2a. Yield: 37%. 2a was synthesized following the general procedure to afford an orange-red solid.  $\delta_{\text{H}}$  (500 MHz,  $\text{CDCl}_3$ ): 3.45 (d, 1H,  $J = 9.06$  Hz), 6.73 (d, 1H,  $J = 9.07$  Hz), 7.22 (t, 1H,  $J = 7.34$  Hz), 7.30 (t, 2H,  $J = 7.60$ ), 7.40 (d, 2H,  $J = 7.55$  Hz), 7.45–7.56 (m, 3H), 7.98 (d, 2H,  $J = 7.06$  Hz).  $\delta_{\text{C}}$  (125 MHz,  $\text{CDCl}_3$ ): 62.3 (CH), 74.3 (CH), 126.6 (CH), 126.8 (CH), 127.1 (CH), 128.9 (CH), 131.5 (CH), 133.7 (4°), 138.0 (4°), 138.8 (4°).  $m/z$  (FAB) 207 (M – (Fe(CO)<sub>3</sub>), 26%), 264 (M – (3 × (CO)), 100%), 293 (M – (2 × (CO)), 10%), 321 (M – (1 × (CO)), 21%), 349 (MH<sup>+</sup>, 44%), 417 (M – (3 × (CO)) + NOBA), 93%). IR (KBr): 2067, 2007, 1990, 1976, 1475, 1456, 1366, 1353, 1261. IR ( $\text{CH}_2\text{Cl}_2$ ): 2067, 2009, 1989. Anal. Found: C, 61.58; H, 3.70. C<sub>18</sub>H<sub>12</sub>FeO<sub>4</sub> requires: C, 62.10; H, 3.47.

$\eta^4$ -((E)-3-(4-Dimethylaminophenyl)-1-phenyl-2-propen-1-one)-tricarbonyliron(0), 2b. Yield: 10%. 2b was synthesized following the general procedure to afford an orange-red solid.  $\delta_{\text{H}}$  (500 MHz,  $\text{CDCl}_3$ ): 2.97 (s, 6H), 3.59 (d, 1H,  $J = 9.21$  Hz), 6.66 (d, 2H,  $J = 8.19$  Hz), 6.72 (d, 1H,  $J = 9.13$  Hz), 7.32 (d, 2H,  $J = 8.10$  Hz), 7.45–7.54 (m, 3H), 7.98 (d, 2H,  $J = 6.92$  Hz).  $\delta_{\text{C}}$  (125 MHz,  $\text{CDCl}_3$ ): 40.3 (2 × CH<sub>3</sub>), 65.7 (CH), 74.5 (CH), 112.5 (CH), 125.6 (4°), 126.5 (CH), 128.0 (CH), 128.8 (CH), 131.1 (CH), 134.3 (4°), 135.6 (4°), 149.7 (4°).  $m/z$  (FAB): 251 (M – (Fe(CO)<sub>3</sub>), 46%), 307 (M – (3 × (CO)), 67%), 324 (MNH<sub>4</sub><sup>+</sup> – (3 × (CO)), 43%), 335 (M – (2 × (CO)), 29%), 364 (M – (1 × (CO)), 16%), 392 (MH<sup>+</sup>, 17%), 460 (M – (3 × (CO)) + NOBA), 43%). IR (KBr): 2047, 1992, 1961, 1606, 1526, 1503, 1476, 1445.6, 1353, 1165. IR ( $\text{CH}_2\text{Cl}_2$ ): 2061, 2001, 1982. Anal. Found: C, 61.48; H, 4.52; N, 4.52. C<sub>20</sub>H<sub>17</sub>FeNO<sub>4</sub> requires: C, 61.41; H, 4.38; N, 3.58.

$\eta^4$ -((E)-3-(4-Methoxyphenyl)-1-phenyl-2-propen-1-one)-tricarbonyliron(0), 2c. Yield: 30%. 2c was synthesized following the general procedure to afford an orange-red solid.  $\delta_{\text{H}}$  (500 MHz,  $\text{CDCl}_3$ ): 3.51 (d, 1H,  $J = 9.15$  Hz), 3.81 (s, 3H), 6.70 (d, 1H,  $J = 9.16$  Hz), 6.86 (d, 2H,  $J = 8.60$  Hz), 7.36 (d, 2H,  $J = 8.59$  Hz), 7.46–7.56 (m, 3H), 7.98 (d, 2H,  $J = 7.25$  Hz).  $\delta_{\text{C}}$  (125 MHz,  $\text{CDCl}_3$ ): 55.3 (CH<sub>3</sub>), 63.2 (CH), 74.4 (CH), 114.5 (CH), 126.5 (CH), 128.1 (CH), 128.9 (CH), 130.7 (4°), 131.4 (CH), 133.9 (4°), 136.9 (4°), 158.9 (4°).  $m/z$  (FAB): 239 (M – (Fe(CO)<sub>3</sub>), 33%), 294 (M – (3 × (CO)), 83%), 311 (MNH<sub>4</sub><sup>+</sup> – (3 × (CO)), 100%), 323 (M – (2 × (CO)), 16%), 351 (M – (1 × (CO)), 20%), 379 (MH<sup>+</sup>, 26%), 447 (M – (3 × (CO)) + NOBA), 63%). IR (KBr): 2069, 2008, 1990, 1980, 1609, 1519, 1474, 1365, 1177, 1034. IR ( $\text{CH}_2\text{Cl}_2$ ): 2065, 2005, 1986. Anal. Found: C, 60.33; H, 4.07. C<sub>19</sub>H<sub>14</sub>FeO<sub>5</sub> requires: C, 60.35; H, 3.73.

$\eta^4$ -((*E*)-3-(4-Methylthiophenyl)-1-phenyl-2-propen-1-one)tricarbonyliron(0), **2d**. Yield: 14%. **2d** was synthesized following the general procedure to afford an orange-red solid.  $\delta_{\text{H}}$  (500 MHz,  $\text{CDCl}_3$ ): 2.49 (s, 3H), 3.44 (d, 1H,  $J = 9.08$  Hz), 6.71 (d, 1H,  $J = 9.08$  Hz), 7.19 (d, 1H,  $J = 8.36$  Hz), 7.34 (d, 2H,  $J = 8.36$  Hz), 7.47–7.58 (m, 3H), 7.97–8.00 (m, 2H).  $\delta_{\text{C}}$  (125 MHz,  $\text{CDCl}_3$ ): 15.6 ( $\text{CH}_3$ ), 62.2 (CH), 74.0 (CH), 126.6 (CH), 126.8 (CH), 127.2 (CH), 128.9 (CH), 131.5 (CH), 133.6 ( $4^\circ$ ), 135.5 ( $4^\circ$ ), 137.6 ( $4^\circ$ ), 137.7 ( $4^\circ$ ).  $m/z$  (FAB): 255 (M – (Fe(CO) $_3$ ), 28%), 310 (M – (3  $\times$  (CO)), 47%), 327 ( $\text{MNH}_4^+$  – (3  $\times$  (CO)), 67%), 338 (M – (2  $\times$  (CO)), 10%), 367 (M – (1  $\times$  (CO)), 17%), 395 (MH $^+$ , 20%), 463 (M – (3  $\times$  (CO)) + NOBA, 64%). IR (KBr): 2067, 1995, 1983, 1597, 1498, 1469, 1453, 1408, 1363, 1097. IR ( $\text{CH}_2\text{Cl}_2$ ): 2067, 2008, 1988. Anal. Found: C, 57.47; H, 3.97.  $\text{C}_{19}\text{H}_{14}\text{FeSO}_4$  requires: C, 57.89; H, 3.58.

$\eta^4$ -((*E*)-3-(4-Chlorophenyl)-1-phenyl-2-propen-1-one)tricarbonyliron(0), **2e**. Yield: 37%. **2e** was synthesized following the general procedure to afford an orange-red solid.  $\delta_{\text{H}}$  (500 MHz,  $\text{CDCl}_3$ ): 3.39 (d, 1H,  $J = 8.99$  Hz), 6.68 (d, 1H,  $J = 8.99$  Hz), 7.28 (d, 2H,  $J = 8.53$  Hz), 7.34 (d, 2H,  $J = 8.52$  Hz), 7.47–7.58 (m, 3H), 7.98 (d, 2H,  $J = 7.13$  Hz).  $\delta_{\text{C}}$  (125 MHz,  $\text{CDCl}_3$ ): 60.7 (CH), 73.7 (CH), 126.6 (CH), 127.9 (CH), 128.9 (CH), 129.1 (CH), 131.7 (CH), 132.7 ( $4^\circ$ ), 133.3 ( $4^\circ$ ), 137.5 ( $4^\circ$ ), 138.5 ( $4^\circ$ ).  $m/z$  (FAB): 243 (M – (Fe(CO) $_3$ ), 14%), 298 (M – (3  $\times$  (CO)), 38%), 315 ( $\text{MNH}_4^+$  – (3  $\times$  (CO)), 63%), 326 (M – (2  $\times$  (CO)), 11%), 355 (M – (1  $\times$  (CO)), 11%), 383 (MH $^+$ , 30%), 451 (M – (3  $\times$  (CO)) + NOBA, 68%). IR (KBr): 2073, 2014, 1990, 1498, 1470, 1454, 1410, 1365, 1096, 1014. IR ( $\text{CH}_2\text{Cl}_2$ ): 2069, 2011, 1990.

$\eta^4$ -((*E*)-3-(4-Bromophenyl)-1-phenyl-2-propen-1-one)tricarbonyliron(0), **2f**. Yield: 20%. **2f** was synthesized following the general procedure to afford an orange-red solid.  $\delta_{\text{H}}$  (500 MHz,  $\text{CDCl}_3$ ): 3.35 (d, 1H,  $J = 8.95$  Hz), 6.65 (d, 1H,  $J = 8.96$  Hz), 7.24 (m, 1H), 7.41 (d, 2H,  $J = 8.30$  Hz), 7.44–7.58 (m, 3H), 7.96 (d, 2H,  $J = 7.38$  Hz).  $\delta_{\text{C}}$  (125 MHz,  $\text{CDCl}_3$ ): 60.7 (CH), 73.6 (CH), 120.8 ( $4^\circ$ ), 126.7 (CH), 128.2 (CH), 129.0 (CH), 131.7 (CH), 132.1 (CH), 133.3 ( $4^\circ$ ), 138.1 ( $4^\circ$ ), 138.7 ( $4^\circ$ ).  $m/z$  (FAB): 289 (M – (Fe(CO) $_3$ ), 17%), 342 (M – (3  $\times$  (CO)), 10%), 427/429 ( $\text{Br}^{79}/\text{Br}^{81}$  MH $^+$ , 9%), 495/497 ( $\text{Br}^{79}/\text{Br}^{81}$  M – (3  $\times$  (CO)) + NOBA, 23%). IR (KBr): 2070, 2010, 1989, 1470, 1454, 1405, 1365, 1010. IR ( $\text{CH}_2\text{Cl}_2$ ): 2069, 2011, 1990. Anal. Found: C, 50.26; H, 2.65.  $\text{C}_{18}\text{H}_{11}\text{FeBrO}_4$  requires: C, 50.63; H, 2.60.

$\eta^4$ -((*E*)-3-(4-Trifluoromethylphenyl)-1-phenyl-2-propen-1-one)tricarbonyliron(0), **2g**. Yield 21%. **2g** was synthesized following the general procedure to afford an orange-red solid.  $\delta_{\text{H}}$  (500 MHz,  $\text{CDCl}_3$ ): 3.40 (d, 1H,  $J = 8.72$  Hz), 6.72 (d, 1H,  $J = 8.77$  Hz), 7.45–7.62 (m, 7H), 8.00 (d, 2H,  $J = 7.14$  Hz).  $\delta_{\text{C}}$  (125 MHz,  $\text{CDCl}_3$ ): 59.5 (CH), 73.4 (CH), 124.12 ( $4^\circ$ , q, 272 Hz), 125.9 (CH, q,  $J = 3.7$  Hz), 126.7 (CH), 126.8 (CH), 128.8 ( $4^\circ$ , q,  $J = 32.5$  Hz), 129.0 (CH), 131.9 (CH), 133.0 ( $4^\circ$ ), 139.5 ( $4^\circ$ ), 143.3 ( $4^\circ$ ).  $m/z$  (FAB) 277 (M – (Fe(CO) $_3$ ), 14%), 332 (M – (3  $\times$  (CO)), 54%), 349 ( $\text{MNH}_4^+$  – (3  $\times$  (CO)), 32%), 361 (M – (2  $\times$  (CO)), 12%), 389 (M – (1  $\times$  (CO)), 14%), 417 (MH $^+$ , 30%), 485 (M – (3  $\times$  (CO)) + NOBA, 65%); IR (KBr) 2079, 2015, 1993, 1982, 1612, 1477, 1454, 1323, 1152, 1126, 1106, 1064, 1014; IR ( $\text{CH}_2\text{Cl}_2$ ) 2071, 2013, 1992, Found C, 54.86; H, 2.87,  $\text{C}_{19}\text{H}_{11}\text{FeF}_3\text{O}_4$  requires C, 54.84; H, 2.66.

$\eta^4$ -((*E*)-3-(3-Methoxyphenyl)-1-phenyl-2-propen-1-one)tricarbonyliron(0), **2h**. Yield: 35%. **2h** was synthesized following the general procedure to afford an orange-red solid.  $\delta_{\text{H}}$  (500 MHz,  $\text{CDCl}_3$ ): 3.42 (d, 1H,  $J = 9.02$  Hz), 3.83 (s, 3H), 6.72 (d, 1H,  $J = 9.02$  Hz), 6.79 (dd, 1H,  $J = 8.20, 1.98$  Hz), 6.94 (s, 1H), 7.02 (d, 1H,  $J = 7.67$  Hz), 7.23 (t, 1H,  $J = 7.93$  Hz), 7.47–7.57 (m, 3H), 7.99 (d, 2H,  $J = 7.11$  Hz).  $\delta_{\text{C}}$  (125 MHz,  $\text{CDCl}_3$ ): 55.3 ( $\text{CH}_3$ ), 62.2 (CH), 74.3 (CH), 112.4 (CH), 112.7 (CH), 119.3 (CH), 126.6 (CH), 128.9 (CH), 129.9 (CH), 131.5 (CH), 133.6 ( $4^\circ$ ), 137.9 ( $4^\circ$ ), 140.3 ( $4^\circ$ ), 156.0 ( $4^\circ$ ).  $m/z$  (FAB): 239 (M – (Fe(CO) $_3$ ), 25%), 294 (M – (3  $\times$  (CO)), 100%), 311 ( $\text{MNH}_4^+$  – (3  $\times$  (CO)), 89%),

322 (M – (2  $\times$  (CO)), 10%), 351 (M – (1  $\times$  (CO)), 22%), 379 (MH $^+$ , 37%), 447 (M – (3  $\times$  (CO)) + NOBA, 76%). IR (KBr): 2064, 2007, 1977, 1607, 1580, 1483, 1447, 1267, 1049. IR ( $\text{CH}_2\text{Cl}_2$ ): 2068, 2009, 1989. Anal. Found: C, 60.54; H, 4.11.  $\text{C}_{19}\text{H}_{14}\text{FeO}_5$  requires: C, 60.35; H, 3.73.

$\eta^4$ -((*E*)-3-(3-Trifluoromethylphenyl)-1-phenyl-2-propen-1-one)tricarbonyliron(0), **2i**. Yield 32%. **2i** was synthesized following the general procedure to afford an orange-red solid.  $\delta_{\text{H}}$  (500 MHz,  $\text{CDCl}_3$ ): 3.41 (d, 1H,  $J = 8.89$  Hz), 6.72 (d, 1H,  $J = 8.89$  Hz), 7.44 (t, 1H,  $J = 7.65$  Hz), 7.46–7.54 (m, 3H), 7.54–7.63 (m, 3H), 8.01 (d, 2H,  $J = 7.12$  Hz).  $\delta_{\text{C}}$  (125 MHz,  $\text{CDCl}_3$ ): 59.8 (CH), 73.4 (CH), 122.9 (CH, q,  $J = 3.7$  Hz), 123.5 (CH, q,  $J = 3.6$  Hz), 125.0 ( $4^\circ$ ), 126.7 (CH), 129.0 (CH), 129.4 (CH), 130.1 (CH), 131.4 ( $4^\circ$ , q,  $J = 33.2$  Hz), 131.8 (CH), 133.0 ( $4^\circ$ ), 139.4 ( $4^\circ$ ), 140.3 ( $4^\circ$ ).  $m/z$  (FAB) 277 (M – (Fe(CO) $_3$ ), 12%), 332 (M – (3  $\times$  (CO)), 54%), 361 (M – (2  $\times$  (CO)), 11%), 389 (M – (1  $\times$  (CO)), 12%), 417 (MH $^+$ , 27%), 485 (M – (3  $\times$  (CO)) + NOBA, 55%); IR (KBr) 2068, 1995, 1455, 1434, 1366, 1357, 1325, 1225, 1167, 1124, 1069; IR ( $\text{CH}_2\text{Cl}_2$ ) 2071, 2013, 1992. Found C, 54.96; H, 2.66,  $\text{C}_{19}\text{H}_{11}\text{FeF}_3\text{O}_4$  requires C, 54.84; H, 2.66.

$\eta^4$ -((*E*)-3-(2-Trifluoromethylphenyl)-1-phenyl-2-propen-1-one)tricarbonyliron(0), **2j**. Yield: 36%. **2j** was synthesized following the general procedure to afford an orange-red solid.  $\delta_{\text{H}}$  (500 MHz,  $\text{CDCl}_3$ ): 3.53 (d, 1H,  $J = 8.67$  Hz), 6.70 (d, 1H,  $J = 8.73$  Hz), 7.32 (t, 1H,  $J = 7.58$  Hz), 7.38 (d, 1H,  $J = 7.95$  Hz), 7.44–7.54 (m, 3H), 7.54–7.59 (m, 1H), 7.67 (d, 1H,  $J = 7.84$  Hz), 8.01 (d, 2H,  $J = 7.29$  Hz).  $\delta_{\text{C}}$  (125 MHz,  $\text{CDCl}_3$ ): 55.4 (CH), 75.1 (CH), 125.9 (CH), 126.4 (CH), 126.8 (CH), 128.7 (CH), 129.0 (CH), 131.7 (CH), 131.9 (CH), 133.0 ( $4^\circ$ ), 138.2 ( $4^\circ$ ), 140.2 ( $4^\circ$ ), 208.6 (br, 3  $\times$  Fe(CO)). The  $\text{CF}_3$  and *ipso* carbons could not be observed even after extended acquisition times.  $m/z$  (FAB): 277 (M – (Fe(CO) $_3$ ), 20%), 333 (M – (3  $\times$  (CO)), 30%), 361 (M – (2  $\times$  (CO)), 22%), 389 (M – (1  $\times$  (CO)), 24%), 417 (MH $^+$ , 47%), 485 (M – (3  $\times$  (CO)) + NOBA, 35%). IR (KBr): 2070, 2014, 1983, 1463, 1374, 1355, 1313, 1274, 1143, 1127, 1102, 1036. IR ( $\text{CH}_2\text{Cl}_2$ ): 2073, 2016, 1990. Anal. Found: C, 54.77; H, 2.83.  $\text{C}_{19}\text{H}_{11}\text{FeF}_3\text{O}_4$  requires: C, 54.84; H, 2.66.

$\eta^4$ -((*E*)-3-(2-Fluorophenyl)-1-phenyl-2-propen-1-one)tricarbonyliron(0), **2k**. Yield: 28%. **2k** was synthesized following the general procedure to afford an orange-red solid.  $\delta_{\text{H}}$  (500 MHz,  $\text{CDCl}_3$ ): 3.58 (d, 1H,  $J = 9.12$  Hz), 6.84 (d, 1H,  $J = 9.13$  Hz), 7.13–7.02 (m, 2H), 7.22 (dd, 1H,  $J = 12.98, 6.43$  Hz), 7.38 (t, 1H,  $J = 7.47$ ), 7.48–7.58 (m, 3H), 8.00 (d, 2H,  $J = 7.31$  Hz).  $\delta_{\text{C}}$  (125 MHz,  $\text{CDCl}_3$ ): 53.7 (CH, d,  $J = 4.41$  Hz), 73.4 (CH, d,  $J = 3.9$  Hz), 115.9 (CH, d,  $J = 22.1$  Hz), 124.3 (CH, d,  $J = 3.5$  Hz), 126.7 (CH), 126.8 (CH, d,  $J = 3.4$  Hz), 126.9 ( $4^\circ$ ), 128.3 (CH, d,  $J = 8.5$  Hz), 128.9 (CH), 131.6 (CH), 133.4 ( $4^\circ$ ), 138.9 ( $4^\circ$ ), 160.8 ( $4^\circ$ , d,  $J = 249$  Hz).  $m/z$  (FAB): 227 (M – (Fe(CO) $_3$ ), 19%), 282 (M – (3  $\times$  (CO)), 47%), 299 ( $\text{MNH}_4^+$  – (3  $\times$  (CO)), 100%), 311 (M – (2  $\times$  (CO)), 24%), 339 (M – (1  $\times$  (CO)), 26%), 367 (MH $^+$ , 57%), 435 (M – (3  $\times$  (CO)) + NOBA, 100%). IR (KBr): 2075, 2071, 2009, 1988, 1978, 1507, 1497, 1465, 1456, 1368, 1354, 1239. IR ( $\text{CH}_2\text{Cl}_2$ ): 2070, 2012, 1990. Anal. Found: C, 59.17; H, 3.26.  $\text{C}_{18}\text{H}_{11}\text{FeFO}_4$  requires: C, 59.05; H, 3.03.

$\eta^4$ -((*E*)-3-(2-Chlorophenyl)-1-phenyl-2-propen-1-one)tricarbonyliron(0), **2l**. Yield: 35%. **2l** was synthesized following the general procedure to afford an orange-red solid.  $\delta_{\text{H}}$  (500 MHz,  $\text{CDCl}_3$ ): 3.80 (d, 1H,  $J = 9.05$  Hz), 6.73 (d, 1H,  $J = 9.05$  Hz), 7.16 (dt, 1H,  $J = 7.63, 1.51$  Hz), 7.21 (t, 1H,  $J = 7.08$  Hz), 7.32 (dd, 1H,  $J = 7.73, 1.18$  Hz), 7.41 (dd, 1H,  $J = 7.80, 1.15$  Hz), 7.48–7.59 (m, 3H), 8.01 (d, 2H,  $J = 7.18$  Hz).  $\delta_{\text{C}}$  (125 MHz,  $\text{CDCl}_3$ ): 56.3 (CH), 73.1 (CH), 125.1 (CH), 126.8 (CH), 126.8 (CH), 127.7 (CH), 128.9 (CH), 130.4 (CH), 131.7 (CH), 133.3 ( $4^\circ$ ), 134.7 ( $4^\circ$ ), 136.8 ( $4^\circ$ ), 139.9 ( $4^\circ$ ).  $m/z$  (FAB): 242 (M – (Fe(CO) $_3$ ), 14%), 298 (M – (3  $\times$  (CO)), 82%), 327 (M – (2  $\times$  (CO)), 29%), 354 (M – (1  $\times$  (CO)), 15%), 383/385 ( $\text{Cl}^{35}/\text{Cl}^{37}$  MH $^+$ , 49%), 451/453 (M – (3  $\times$  (CO)) + NOBA, 33%). IR (KBr): 2066, 2007,

1985, 1488, 1455, 1365, 1349, 1037. IR (CH<sub>2</sub>Cl<sub>2</sub>): 2071, 2013, 1990. Anal. Found: C, 54.93; H, 3.09. C<sub>18</sub>H<sub>11</sub>FeClO<sub>4</sub> requires: C, 56.57; H, 2.90.

**$\eta^4$ -(*E*)-3-(3,4,5-Trimethoxyphenyl)-1-phenyl-2-propen-1-one-tricarbonyliron(0), 2m.** Yield: 13%. **2m** was synthesized following the general procedure to afford an orange-red solid.  $\delta_{\text{H}}$  (500 MHz, CDCl<sub>3</sub>): 3.37 (d, 1H, *J* = 8.53 Hz), 3.86 (s, 3H), 3.88 (s, 6H), 6.61 (s, 2H), 6.65 (d, 1H, *J* = 8.93 Hz), 7.66–7.44 (m, 3H), 7.99 (d, 2H, *J* = 6.45 Hz).  $\delta_{\text{C}}$  (125 MHz, CDCl<sub>3</sub>): 56.2 (CH<sub>3</sub>), 60.9 (CH<sub>3</sub>), 63.3 (CH), 74.3 (CH), 104.1 (CH), 120.0 (4°), 126.7 (CH), 128.9 (CH), 131.5 (CH), 133.6 (4°), 134.3 (4°), 137.7 (4°), 153.6 (4°). *m/z* (FAB): 298 (M – (Fe(CO)<sub>3</sub>), 35%), 354 (M – (3×(CO)), 58%), 382 (M – (2×(CO)), 13%), 411 (M – (1×(CO)), 28%), 439 (MH<sup>+</sup>, 27%), 507 (M – (3×(CO)) + NOBA), 38%). IR (KBr): 2060, 2005, 1971, 1587, 1512, 1479, 1456, 1420, 1372, 1322, 1279, 1245, 1128, 1006. IR (CH<sub>2</sub>Cl<sub>2</sub>): 2067, 2008, 1987. Anal. Found: C, 59.64; H, 5.18. C<sub>21</sub>H<sub>18</sub>FeO<sub>7</sub>·0.5C<sub>6</sub>H<sub>14</sub> requires: C, 60.02; H, 5.04.

**$\eta^4$ -(*E*)-3-(2,4,6-Trimethylphenyl)-1-phenyl-2-propen-1-one-tricarbonyliron(0), 2n.** Yield: 13%. **2n** was synthesized following the general procedure to afford an orange-red solid.  $\delta_{\text{H}}$  (300 MHz, CDCl<sub>3</sub>): 2.17 (s, 3H), 2.53 (s, 6H), 3.57 (d, 1H, *J* = 10.26 Hz), 6.78–6.80 (m, 2H), 7.18 (t, 1H, *J* = 5.40 Hz), 7.41–7.48 (m, 3H), 7.80–7.93 (m, 2H).  $\delta_{\text{C}}$  (125 MHz, CDCl<sub>3</sub>): 20.8 (CH<sub>3</sub>), 22.9 (CH<sub>3</sub>), 64.1 (CH), 76.3 (CH), 126.6, 128.9, 131.0, 131.5, 131.7, 133.9, 136.7, 136.9, 138.1. *m/z* (FAB): 251 (M – (Fe(CO)<sub>3</sub>), 28%), 306 (M – (3×(CO)), 100%), 323 (MNH<sub>4</sub><sup>+</sup> – (3×(CO)), 48%), 334 (M – (2×(CO)), 7%), 363 (M – (1×(CO)), 16%), 391 (MH<sup>+</sup>,

11%), 459 (M – (3×(CO)) + NOBA), 52%). IR (KBr): 2055, 1990, 1982, 1977, 1962, 1659, 1602, 1261, 1096, 1024. IR (CH<sub>2</sub>Cl<sub>2</sub>): 2062, 2001, 1985.

**X-ray Crystallography.** Diffraction data were collected at 110 K on a Bruker Smart Apex diffractometer with Mo K $\alpha$  radiation ( $\lambda$  = 0.71073 Å) using a SMART CCD camera. Diffractometer control, data collection, and initial unit cell determination was performed using SMART (v5.625 Bruker-AXS). Frame integration and unit-cell refinement software was carried out with SAINT+ (v6.22, Bruker AXS). Absorption corrections were applied by SADABS (v2.03, Sheldrick). Structures were solved by direct methods using SHELXS-97 (Sheldrick, 1990) and refined by full-matrix least-squares using SHELXL-97 (Sheldrick, 1997). All non-hydrogen atoms were refined anisotropically. Hydrogen atoms were placed using a “riding model” and included in the refinement at calculated positions.

**Acknowledgment.** We gratefully acknowledge the financial support of the EPSRC and University of York. I.J.S.F. thanks the Royal Society for a University Research Fellowship and generous equipment grant, and Astra-Zeneca for an unrestricted research award.

**Supporting Information Available:** Crystallographic information files (CIF) for **1i**, **1m**, **2a**, **2g**, **2i**, **2j**, **2k**, and **2l**. This material is available via the Internet free of charge at <http://pubs.acs.org>.

OM7006425